Structural Engineering and Mechanics, *Vol. 73, No. 4 (2020) 407-426*
DOI: https://doi.org/10.12989/sem.2020.73.4.407

A semi-analytical mesh-free method for 3D free vibration analysis of bi-directional FGP circular structures subjected to temperature variation

Mahnaz Shamshirsaz*[1], Shahin Sharafi[1a], Javad Rahmatian[1,2a], Sajad Rahmatian[1,3a] and Naserodin Sepehry[1,4b]

[1]*New Technologies Research Center, Amirkabir University of Technology, 424 Hafez Ave, 15875-4413, Tehran, Islamic Republic of Iran*
[2]*Department of Mechanical Engineering, Razi University of Kermanshah, Tagh Bostan, 67144-15111, Kermanshah, Islamic Republic of Iran*
[3]*Department of Mechanical Engineering, University of Tehran, 16th Azar St., Enghelab Sq, 1417466191, Tehran, Islamic Republic of Iran*
[4]*Faculty of Mechanical and Mechatronics Engineering, Shahrood University of Technology, Shahrood, 3619995161, Islamic Republic of Iran*

(Received May 8, 2019, Revised August 3, 2019, Accepted October 15, 2019)

Abstract. In this present paper, a semi-analytical mesh-free method is employed for the three-dimensional free vibration analysis of a bi-directional functionally graded piezoelectric circular structure. The dependent variables have been expanded by Fourier series with respect to the circumferential direction and have been discretized through radial and axial directions based on the mesh-free shape function. The current approach has a distinct advantage. The nonlinear Green-Lagrange strain is employed as the relationship between strain and displacement fields to observe thermal impacts in stiffness matrices. Nevertheless, high order terms have been neglected at the final steps of equations driving. The material properties are assumed to vary continuously in both radial and axial directions simultaneously in accordance with a power law distribution. The convergence and validation studies are conducted by comparing our proposed solution with available published results to investigate the accuracy and efficiency of our approach. After the validation study, a parametric study is undertaken to investigate the temperature effects, different types of polarization, mechanical and electric boundary conditions and geometry parameters of structures on the natural frequencies of functionally graded piezoelectric circular structures.

Keywords: 3D free vibration; functionally graded piezoelectric circular structures; nonlinear Green-Lagrange strain; mesh-free method; semi-analytical method

1. Introduction

Piezoelectric materials have attracted many attentions in recent decades due to their inherent properties which mainly are used in engineering applications such as electro-mechanical systems and energy harvesting (Priya and Inman 2009). However, traditional laminated piezoelectric structures have some shortcomings such as delamination, cracking at low temperature, creeping at high temperatures (Zhu and Meng 1995). Also, abrupt changing in material properties at interfaces can cause stress concentration which may deteriorate performance of systems and reduce lifetime and reliability of piezoelectric devices (Kruusing 2000; Qiu, Tani *et al*. 2003). In order to overcome these problems, the concept of functionally graded materials (FGM) which has been presented by Koizumie (Koizumi 1997), attracts many researchers to model the smoother structures to avoid such drawbacks. In FGM structures, the properties of materials vary continuously and gradually in one or more directions which yield better performance than the multilayer composites. Nguyen and Tran (Nguyen and Tran 2018) developed a free of shear locking finite element model to study free vibration of tapered bidirectional functionally graded material beams. Benlahcen *et al*. (Benlahcen, Belakhdar *et al*. 2018) derived an analytical formulation to investigate the thermal buckling resistance of FGM plates expose to uniform and gradient temperature changes. The combination of piezoelectric materials and FGM concept emerge a new class of materials which known as functionally graded piezoelectric (FGP) materials. These materials by presenting the continuous variation of electro-mechanical properties at especial directions, reduce significant abrupt changing and stress concentrations (Zhu and Meng 1995; Wu, Kahn *et al*. 1996; Lezgy-Nazargah, Vidal *et al*. 2013); therefore, owing to these significant advantages of FGP materials, the functionally graded piezoelectric materials are used in many different fields (Almajid, Taya *et al*. 2002). Larkin and Abdelkefi (Larkin and Abdelkefi 2019) studied behavior of single-layered functionally graded piezoelectric energy harvesting systems. In their work, they determined whether the central axis representation can model a single-layered FGP energy harvester or not. Due to optimize the utilization of these smart materials, it is necessary to have a comprehensive understanding about different behaviors of FGP structures in different environments. There are several researches that offer a variety of methods to achieve this goal. Wang *et al*. (Wang, Xu *et al*. 2010) employed an exact solution for analyzing FGP circular plate based on three-dimensional

*Corresponding author, Ph.D. Professor
E-mail: shamshir@aut.ac.ir
[a] M. Sc
[b] Ph.D.

Copyright © 2020 Techno-Press, Ltd.

ISSN: 1225-4568 (Print), 1598-6217 (Online)

theory of piezoelectricity. An analytical solution for investigation of buckling of FGP rectangular plate based on high-order shear deformation plate theory was presented by Ghasemabadian and Kadkhodayan (Ghasemabadian and Kadkhodayan 2016). They derived the equilibrium equations of the plate using principle of minimum total potential energy. Tsai and Wu (Tsai and Wu 2008) presented the method of multiple time scale for investigating free vibration of simply supported, doubly curved functionally graded magneto-electro-elastic shells with open circuit surface conditions. Also, they presented two asymptotic formulations for the cylindrical bending vibration of simply supported FGP cylindrical shells by using 3D piezoelectricity and perturbation method (Wu and Tsai 2009). electromagnetothermoelastic behaviors of an FGP hollow sphere was assessed by Dai and Rao (Dai and Rao 2011). Their structure had been placed in electric and magnetic field and was under thermal and mechanical loads. The goal of their work was designing the optimum FGP spherical structure, and for aiming this goal, they investigated efficient parameters. Bodaghi and Shakri (Bodaghi and Shakeri 2012) employed an analytical method to report results of free vibration and transient response of functionally graded piezoelectric cylindrical panels subjected to impulsive loads. Sheng and Wang (Sheng and Wang 2010) investigated thermos-elastic vibration and buckling of functionally graded cylindrical shell based on first-order shear deformation theory (FSDT). Zhong and Shang (Zhong and Shang 2003) by employing an exact method, investigated 3D analysis of simply supported functionally graded piezoelectric plate. Wu *et al*.(Wu, Shen *et al*. 2003) provided an exact solution for FGP cylindrical shell which are used as sensors and actuators.

Most of the structures have complex figures, and mostly it is impossible to model them by pure analytical methods to predict structures behaviors. Numerical methods, especially the finite element method (FEM) can play a significant role for solving this problem. Bodaghi *et al*. (Bodaghi, Damanpack *et al*. 2012) investigated non-linear active control of dynamic response of functionally graded beam in thermal environment exposed to blast loading. They considered two FGP layers bonded to the beam surfaces as actuator and sensor. They derived non-linear equation of motion based on the first-order shear deformation theory and von Karman geometrical nonlinearity. Finally, they utilized generalized differential quadrature technique to solve the governing equations. Xiong and Tian (Xiong and Tian 2017) applied finite element method to investigate transient thermos-piezo-elastic response of functionally graded piezoelectric plate. Behjat and Khoshravan (Behjat and Khoshravan 2012) presented response of FGP plate subjected to mechanical and electrical loads by conducting nonlinear FEM. Amini *et al*. (Amini, Emdad *et al*. 2015) developed a finite element method to simulate the functionally graded piezoelectric harvester in unimorph and biomorph configurations. Also, Behjat *et al*. (Behjat, Salehi *et al*. 2009) investigated free vibration and dynamic response of FGP panels by FEM using four-node elements. On the other hand, using pure numerical method has high costs in computations, especially for three-dimensional analysis. Based on this reason, recently, most researchers have turned to semi analytical methods which can obtain more accurate results with less computing. A comprehensive review paper about the development of different semi-analytical methods is provided by Wu and Liu (Wu and Liu 2016). In their work, they conducted a comparative study of the results obtained by using different semi-analytical methods. Khayat *et al*. (Khayat, Dehghan *et al*. 2018) applied the semi-analytical finite strip method to examine the free vibration of cylindrical shell made up of functionally graded materials. Wu and Haung (Wu and Huang 2019) analyzed 3D stress and deformation of bi-directional FG truncated conical shell by developing Reissner's mixed variational theorem (RMVT) based finite annular prism method (FAPM). They considered combination of boundary conditions for their investigations. Wu and Li (Wu and Li 2013) extended a RMVT –based finite rectangular prism method for 3D analysis of sandwich FG plate subjected to a sinusoidally or uniformly distributed load. Nie and Zhong (Nie and Zhong 2007) by presenting a state space method combined with one directional differential quadrature method, provided results for 3D vibration analysis of FGP circular plate. Li and Shi (Li and Shi 2009) by using a modified state space method based on a numerical method, analyzed 3D free vibration of an FGPM beam. Liu and Lee (Liu and Lee 2000) reduced three-dimensional finite element method (FEM) to two-dimensional sequence for the vibration of thick circular and annular plate. They employed different displacement field instead of conventional displacement fields. Allahverdizadeh *et al*. (Allahverdizadeh, Naei *et al*. 2008) developed a semi-analytical method for nonlinear behavior of thin circular functionally graded plate. They presented their results in vibration of the structure in thermal environment by using von-Kerman's dynamic equations. Yas and Moluodi (Yas and Moloudi 2015) analyzed 3D free vibration of FGP annular plate by employing a state-space method based on differential quadrature (SSDQM) method. Lu *et al*. (Lü, Lim *et al*. 2009) carried out the SSDGM as a semi-analytical method to investigate multi-directional FGP plate using 3D elasticity theory. Nie and Zhong (Nie and Zhong 2010) conducted the state-space method based on the differential quadrature method to investigate the dynamic analysis of multi-directional functionally graded annular plates.

In recent decades, the mesh-free method has been introduced to omit element dependency in simulations. The meshless or mesh-free method, as a novel and robust class computational method, have been conducted to solving a variety of partial differential equations (PDE) problems in solid and fluid mechanics. Mesh-free methods are classified into three classes according to function approximation schemes: Mesh-free methods based on the moving least squares approximation (MLS), mesh-free methods based on the integral representation method for the function approximation and mesh-free methods based on the point interpolation method (Liu and Gu 2005). As though the finite element methods (FEM) are considered as powerful tools to solve problems in a number of realms, finite element methods encounter many shortcomings in solving

problems which have not been solved yet. There are several significant advantages which mesh-free method overcomes the drawbacks which conventional FEM faced with. Mesh-free methods neglect the predefined meshes in problem domains by introducing arbitrary nodes, which these nodes are scattered in problem domains without no prior relationship between nodes. Having smooth and continuous shape functions is considered as another significant superiority of the mesh-free methods than FEM (Liu and Gu 2005), which leads to obtain more accurate results. These distinguished advantages encourage engineers and researchers to employ the mesh-free methods in problems with complex geometries and fracture problems with moving discontinuous. Chuaqui and Roque (Chuaqui and Roque 2017) used the multi-quadric radial basis function (RBF) as a grid-free method or mesh-free method to describe the electro-mechanical static response of FGP Timoshenko beams. Qian and Batra (Qian and Batra 2005) by carrying out the mesh-free local Petrov-Galerkin (MLPG), studied free and forced vibration of a bi-directional functionally graded cantilever beam. Mikaeeli and Behjat (Mikaeeli and Behjat 2016) employed the three-dimensional Element-Free Galerkin (EFG) method to investigate the static behavior analysis of thick FGP plate. Froutan *et al*. (Foroutan, Mohammadi *et al*. 2017) modeled a FGP cylindrical panel by a three-dimensional mesh-free method. Due to high cost of 3D numerical methods, especially for the mesh-free method in computations, few researchers combined the mesh-free method with analytical methods. Wu and Liu (Wu and Liu 2016) developed state-space differential reproducing kernel method for the 3D analysis of functionally graded axisymmetric circular plate. Wu and Yang (Wu and Yang 2011) employed a semi-analytical element-free Galerkin method for the 3D free vibration analysis of multilayered FGM circular hollow cylinders. In their work, they developed differential reproducing Karnel (DRK) as the interpolation for three-dimensional free vibration analysis of functionally graded hollow cylinder. However, they considered linear relationship between strain and displacement fields to investigate the natural frequencies. Furthermore, they did not study effects of temperature variations on stiffness matrices and so on the natural frequencies.

To the best of the author's knowledge, a semi-analytical mesh-free method based on MLS shape function has not been carried out for three-dimensional free vibration analysis of bi-directional FGP circular structures under temperature variations using nonlinear strain-displacement relationship. In this article, we considered that there is no dependency between temperature variation and material properties to assess purely effects of nonlinear relationship on the natural frequency under temperature variations. Using the linear relationship between displacement field and strain vector leads to neglect thermal effects on the mass and stiffness matrices. Therefore, initially, the nonlinear relationship between displacement and strain fields is used to induce thermal effects on mentioned matrices, and after obtaining this goal, high order terms eliminated to solve the equations linearly. Furthermore, this work has another characteristics. The researchers who combined numerical approaches with analytical approach did not consider pure warping modes, while in this paper has been done. Therefore, the electrical and mechanical field variables have been expanded by Fourier series with respect to the circumferential direction in which both even and odd terms (coefficients of sines and cosine functions) are considered. Alongside the analytical approach, approximation of the field variables with respect to radial and axial direction has been done by a mesh-free method. Due to using the MLS shape function which does not satisfy the Kronecker delta property, the essential boundary condition cannot be imposed directly. The transformation method is conducted to modify the matrices for enforcing essential boundary conditions. Material properties are assumed to vary smoothly through the radial and axial directions simultaneously. After validation and convergence study, the effects of different geometry parameters of circular structures, different types of polarization (electrical boundary conditions) and temperature on the natural frequencies of structures are investigated.

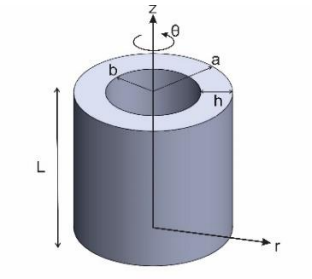

Fig. 1 FGP Circular Structure

2. Material properties

Consider a bi-directional FGP circular structure in the cylindrical coordinate system (r, θ, z) as depicted in Fig. 1, where r, θ and z represent the radial, circumferential and axial directions, respectively. Also, the center of the bottom cylinder is considered as the origin of the cylindrical coordinate-system. Mechanical and electrical properties of FGP cylinder vary continuously through both radial and axial directions. The structure is composed by four different primary piezoelectric materials.

The volume fraction of these materials with (r, θ, z) location is assumed to vary according to the power law function (Asgari and Akhlaghi 2010).

$$\begin{aligned} V_{PZT1} &= \left[1-\left(\frac{r-r_{in}}{r_{out}-r_{in}}\right)^{n_r}\right]\left[1-\left(\frac{z}{L}\right)^{n_z}\right] \\ V_{PZT2} &= \left[1-\left(\frac{r-r_{in}}{r_{out}-r_{in}}\right)^{n_r}\right]\left(\frac{z}{L}\right)^{n_z} \\ V_{PZT3} &= \left(\frac{r-r_{in}}{r_{out}-r_{in}}\right)^{n_r}\left[1-\left(\frac{z}{L}\right)^{n_z}\right] \\ V_{PZT4} &= \left(\frac{r-r_{in}}{r_{out}-r_{in}}\right)^{n_r}\left(\frac{z}{L}\right)^{n_z} \end{aligned} \quad (1)$$

where, V_{PZT-i} $(i = 1,2,3,4)$ is the volume fraction of i_{th}

primary material. n_r and n_z denote the power index for materials distribution in radial and axial directions, respectively, which can be considered from zero to infinite. r_{in}, r_{out} and L demonstrate the inner, outer radius and height of the structure, respectively. The effective properties of the cylinder are calculated based on volume fraction and properties of primary materials by the following equation:

$$P_{eff}(r,z) = P_{PZT1}V_{PZT1} + P_{PZT2}V_{PZT2} + P_{PZT3}V_{PZT3} + P_{PZT4}V_{PZT4} \quad (2)$$

where $P_{eff}(r,z)$ is considered as arbitrary effective material property and P_{PZTi} ($i = 1,2,3,4$) denote corresponding property of i_{th} primary material.

3. Governing equations

3.1 Hamilton principle

The dynamic equations of the structure can be extracted using Hamilton principle as follow:

$$\int_{t_1}^{t_2} \delta KE dt - \int_{t_1}^{t_2} \delta H dt + \int_{t_1}^{t_2} \delta W dt = 0 \quad (3)$$

where KE, H and W are representative of kinetic energy, enthalpy and work done by generalized external loads respectively, and they can be obtained as Eq. (4), (5-a) and (5-b):

$$\delta W = \int (\delta U^T F_{\boldsymbol{b}} + \delta \phi^T Q_b) d\Omega + \int (\delta U^T F_{\boldsymbol{s}} + \delta \phi^T Q_s) dS\,, U = [u \quad v \quad w]^T \quad (4)$$

where U is the displacement vector that contains u, v and w parameters which demonstrate displacement in r, θ and z directions. $F_{\boldsymbol{b}}, Q_b, F_{\boldsymbol{s}}$ and Q_s are the representative of body mechanical forces, body electrical forces, surface mechanical forces and surface electrical forces. Subscripts b and s denote body and surface terms, respectively. The remaining terms of Hamilton principle can be calculated as follow:

$$KE = \int \frac{1}{2} \dot{U}^T \rho \dot{U} d\Omega \rightarrow \int_{t_1}^{t_2} \delta KE dt = -\int_{t_1}^{t_2} \int (\delta U)^T \rho \ddot{U} d\Omega\, dt \quad (5\text{-a})$$

$$H = \int \left(\frac{1}{2} S^T T - \frac{1}{2} E^T D \right) d\Omega \quad (5\text{-b})$$

where E, D, S and T are considered as the electric field vector, electric displacement vector, strain and stress vector respectively which are defined as following equations:

$$T = [\sigma_{rr}, \sigma_{\theta\theta}, \sigma_{zz}, \sigma_{\theta z}, \sigma_{rz}, \sigma_{r\theta}]^T$$
$$S = [\varepsilon_{rr}, \varepsilon_{\theta\theta}, \varepsilon_{zz}, 2\varepsilon_{\theta z}, 2\varepsilon_{rz}, 2\varepsilon_{r\theta}]^T \quad (6)$$
$$E = [E_r, E_\theta, E_z]^T$$
$$D = [D_r, D_\theta, D_z]^T$$

The stress-charge form of piezoelectricity constitutive equations which include thermal effects without consideration of pyroelectric effects can be written as follows:

$$\sigma_{ij} = \mathrm{C}_{ijkl}^E \varepsilon_{kl} - e_{ijk} E_k - \mathrm{C}_{ijkl}^E \alpha_{ij} \Delta T, 1 \le i,j,k,l \le 3$$
$$D_i = \mathrm{e}_{ikl} \varepsilon_{kl} + \xi_{ij}^{\varepsilon} E_j, 1 \le i,j,k,l \le 3 \quad (7)$$

where σ_{ij}, ε_{kl}, E_k, $D_i, C_{ijkl}^E, e_{ijk}, \xi_{ij}^{\varepsilon}$ and α_{ij} are an entry of the stress tensor, strain tensor, electric field vector, electric displacement vector, elastic stiffness matrix, piezoelectric matrix, permittivity dielectric matrix and thermal expansion matrix, respectively. In this paper index 1, 2 and 3 are correspond to r, θ and z independent variables. ΔT presents the temperature difference between the current temperature and the reference temperature (25℃). Thus, the electric displacement vector and the stress vector in Eq. (5-b) can be rewritten as below:

$$T = \mathrm{C}^{\mathrm{E}} S - \mathrm{e}^{\mathrm{T}} E - \mathrm{C}^{\mathrm{E}} \alpha \Delta T$$
$$D = \mathrm{e} S + \xi E \quad (8)$$

As we know the PZT materials are transversely isotropic, so elastic stiffness matrix, piezoelectric matrix, permittivity dielectric matrix and thermal expansion matrix can be defined as bellow. It should be noticed that the electric matrices of axially polarization differ from radially polarization ones.

$$\mathrm{C}^{\mathrm{E}} = \begin{bmatrix} \mathrm{C}_{rrrr}^{\mathrm{E}} & \mathrm{C}_{rr\theta\theta}^{\mathrm{E}} & \mathrm{C}_{rrzz}^{\mathrm{E}} & 0 & 0 & 0 \\ \mathrm{C}_{\theta\theta rr}^{\mathrm{E}} & \mathrm{C}_{\theta\theta\theta\theta}^{\mathrm{E}} & \mathrm{C}_{\theta\theta zz}^{\mathrm{E}} & 0 & 0 & 0 \\ \mathrm{C}_{zzrr}^{\mathrm{E}} & \mathrm{C}_{zz\theta\theta}^{\mathrm{E}} & \mathrm{C}_{zzzz}^{\mathrm{E}} & 0 & 0 & 0 \\ 0 & 0 & 0 & \mathrm{C}_{\theta z\theta z}^{\mathrm{E}} & 0 & 0 \\ 0 & 0 & 0 & 0 & \mathrm{C}_{rzrz}^{\mathrm{E}} & 0 \\ 0 & 0 & 0 & 0 & 0 & \mathrm{C}_{r\theta r\theta}^{\mathrm{E}} \end{bmatrix} \quad (9\text{-a})$$

$$\mathrm{e} = \begin{bmatrix} 0 & 0 & 0 & 0 & \mathrm{e}_{rrz} & 0 \\ 0 & 0 & 0 & \mathrm{e}_{\theta\theta z} & 0 & 0 \\ \mathrm{e}_{zrr} & \mathrm{e}_{z\theta\theta} & \mathrm{e}_{zzz} & 0 & 0 & 0 \end{bmatrix},\ \mathrm{e}_{rrz} = \mathrm{e}_{\theta\theta z}, \mathrm{e}_{zrr} = \mathrm{e}_{z\theta\theta};\ \text{for axial polarization} \quad (9\text{-b})$$

$$\mathrm{e} = \begin{bmatrix} \mathrm{e}_{rrr} & \mathrm{e}_{r\theta\theta} & \mathrm{e}_{rzz} & 0 & 0 & 0 \\ 0 & 0 & 0 & 0 & 0 & \mathrm{e}_{\theta r\theta} \\ 0 & 0 & 0 & 0 & \mathrm{e}_{zrz} & 0 \end{bmatrix}, \mathrm{e}_{zzz} = \mathrm{e}_{\theta\theta z}, \mathrm{e}_{zrz} = \mathrm{e}_{\theta r\theta};\ \text{for radial polarized} \quad (9\text{-c})$$

$$\xi = \begin{bmatrix} \xi_{rr} & 0 & 0 \\ 0 & \xi_{\theta\theta} & 0 \\ 0 & 0 & \xi_{zz} \end{bmatrix}, \xi_{rr} = \xi_{\theta\theta};\ \text{for axial polarized} \quad (9\text{-d})$$

$$\xi = \begin{bmatrix} \xi_{rr} & 0 & 0 \\ 0 & \xi_{\theta\theta} & 0 \\ 0 & 0 & \xi_{zz} \end{bmatrix}, \xi_{zz} = \xi_{\theta\theta};\ \text{for radial polarized} \quad (9\text{-e})$$

$$\alpha = [\alpha_{rr}, \alpha_{\theta\theta}, \alpha_{zz}, 0, 0, 0]^{\mathrm{T}} \quad (9\text{-f})$$

Employing Eq. (8) in Eq. (5-b), the variation of the enthalpy term in Hamilton principle can be expressed by following equation.

$$\delta H = \int (\delta S^T \mathrm{C}^{\mathrm{E}} S - \delta S^T \mathrm{e}^{\mathrm{T}} E - \delta S^T \mathrm{C}^{\mathrm{E}} \alpha \Delta T - \delta E^{\mathrm{T}} \mathrm{e} S - \delta E^T \xi E) d\Omega \quad (10)$$

One of the major aim of this paper is an investigation of the thermal impact on the natural frequencies. The temperature effect appears as the external loads in the dynamic equations and does not have an effect on the stiffness of the structure if the linear relationship was considered between the strain and the displacement. Yet, unlike the linear relationship, the nonlinear one satisfies this goal because of having high order terms, and based on this reason, for observing thermal effects on stiffness matrix, the nonlinear Green-Lagrange Strain relation is employed as Eq. (11).

$$\begin{bmatrix} \varepsilon_{rr} & \varepsilon_{r\theta} & \varepsilon_{rz} \\ \varepsilon_{\theta r} & \varepsilon_{\theta\theta} & \varepsilon_{\theta z} \\ \varepsilon_{zr} & \varepsilon_{z\theta} & \varepsilon_{zz} \end{bmatrix} = \frac{1}{2} * (\begin{bmatrix} 1+\frac{\partial u}{\partial r} & \frac{1}{r}\frac{\partial u}{\partial \theta}-\frac{v}{r} & \frac{\partial u}{\partial z} \\ \frac{\partial v}{\partial r} & 1+\frac{1}{r}\frac{\partial v}{\partial \theta}+\frac{u}{r} & \frac{\partial v}{\partial z} \\ \frac{\partial w}{\partial r} & \frac{1}{r}\frac{\partial w}{\partial \theta} & 1+\frac{\partial w}{\partial z} \end{bmatrix}^{T} * \begin{bmatrix} 1+\frac{\partial u}{\partial r} & \frac{1}{r}\frac{\partial u}{\partial \theta}-\frac{v}{r} & \frac{\partial u}{\partial z} \\ \frac{\partial v}{\partial r} & 1+\frac{1}{r}\frac{\partial v}{\partial \theta}+\frac{u}{r} & \frac{\partial v}{\partial z} \\ \frac{\partial w}{\partial r} & \frac{1}{r}\frac{\partial w}{\partial \theta} & 1+\frac{\partial w}{\partial z} \end{bmatrix} - I) \quad (11)$$

where I is the unique matrix. By obtaining the entries of strain tensor ε_{ij} $(1 \le i,j \le 3)$ from Eq.(11), the strain vector S can be written as the combination of linear operator on the displacement field and second order nonlinear part on displacement field as bellow.

$$S = L_U(r,\theta,z)U + NL_U(r,\theta,z,U) \quad (12)$$

where L_U is considered as the linear operator as follow:

$$L_U = \begin{bmatrix} \frac{\partial}{\partial r} & 0 & 0 \\ \frac{1}{r} & \frac{1}{r}\frac{\partial}{\partial \theta} & 0 \\ 0 & 0 & \frac{\partial}{\partial z} \\ \frac{1}{r}\frac{\partial}{\partial \theta} & \frac{\partial}{\partial r}-\frac{1}{r} & 0 \\ 0 & \frac{\partial}{\partial z} & \frac{1}{r}\frac{\partial}{\partial \theta} \\ \frac{\partial}{\partial z} & 0 & \frac{\partial}{\partial r} \end{bmatrix} \quad (13)$$

And NL_U is described the nonlinear part for the displacement field as bellow:

$$NL_U(r,\theta,z,U)_{(1,1)} = \frac{1}{2}\left(\left(\frac{\partial u}{\partial r}\right)^2 + \left(\frac{\partial v}{\partial r}\right)^2 + \left(\frac{\partial w}{\partial r}\right)^2\right)$$

$$NL_U(r,\theta,z,U)_{(2,1)} = \frac{1}{r^2}\left(u\frac{\partial v}{\partial \theta} - v\frac{\partial u}{\partial \theta}\right) + \frac{1}{2}\left(\frac{u^2}{r^2}+\frac{v^2}{r^2}\right) + \frac{1}{2r^2}\left(\left(\frac{\partial u}{\partial \theta}\right)^2 + \left(\frac{\partial v}{\partial \theta}\right)^2 + \left(\frac{\partial w}{\partial \theta}\right)^2\right) \quad (14)$$

$$NL_U(r,\theta,z,U)_{(3,1)} = \frac{1}{2}\left((\frac{\partial u}{\partial z})^2 + (\frac{\partial v}{\partial z})^2 + (\frac{\partial w}{\partial z})^2\right)$$

$$NL_U(r,\theta,z,U)_{(4,1)} = \frac{1}{2r}\left(u\frac{\partial v}{\partial z} - v\frac{\partial u}{\partial z}\right) + \frac{1}{2r}\left(\frac{\partial u}{\partial \theta}\frac{\partial u}{\partial z} + \frac{\partial v}{\partial \theta}\frac{\partial v}{\partial z} + \frac{\partial w}{\partial \theta}\frac{\partial w}{\partial z}\right)$$

$$NL_U(r,\theta,z,U)_{(5,1)} = \left(\frac{\partial u}{\partial z}\frac{\partial u}{\partial r} + \frac{\partial v}{\partial z}\frac{\partial v}{\partial r} + \frac{\partial w}{\partial z}\frac{\partial w}{\partial r}\right)$$

$$NL_U(r,\theta,z,U)_{(6,1)} = \frac{1}{r}\left(u\frac{\partial v}{\partial r} - v\frac{\partial u}{\partial r}\right) + \frac{1}{r}\left(\frac{\partial u}{\partial \theta}\frac{\partial u}{\partial r} + \frac{\partial v}{\partial \theta}\frac{\partial v}{\partial r} + \frac{\partial w}{\partial \theta}\frac{\partial w}{\partial r}\right)$$

Alongside writing the strain vector S based on the variables of the displacement field, the relation between potential and electrical field for cylindrical coordinate can be obtained through following equation:

$$E = -\nabla\Phi = -\frac{\partial\Phi}{\partial r}\hat{e}_r - \frac{1}{r}\frac{\partial\Phi}{\partial\theta}\hat{e}_\theta - \frac{\partial\Phi}{\partial z}\hat{e}_z \rightarrow E = -L_\Phi\Phi,\ L_\Phi = \begin{bmatrix} \frac{\partial}{\partial r} \\ \frac{1}{r}\frac{\partial}{\partial\theta} \\ \frac{\partial}{\partial z} \end{bmatrix} \quad (15)$$

3.2 Semi-analytical method

Substitution of Eq. (12) and (15) in the terms of Hamilton Principle leads to obtain continuous partial differential equations. Based on this fact that it is either difficult or computationally expensive to derive a pure analytical method or a pure numerical method for such equations with bi-directional non-homogeneity, researchers recently have employed semi-analytical method to solve these kinds of problems. In this paper a particular semi-analytical approach is used which is a combination of Fourier series as an analytical method to expand dependent variables u, v, w with respect to circumferential direction. A modified mesh-free method as a numerical tool is used to approximate the dependent variables through radial and axial directions. In other words, dependent variables are periodic functions with respect to the circumferential direction. So, they can be expanded based on sine and cosine functions as Eq. (16).

$$\begin{aligned} u(r,z,\theta) &= \sum_{n=0}^{Nh}\left[\bar{u}_n(r,z)cos\frac{n\pi}{\Theta}\theta + \bar{\bar{u}}_n(r,z)sin\frac{n\pi}{\Theta}\theta\right] \\ v(r,z,\theta) &= \sum_{n=0}^{Nh}\left[\bar{v}_n(r,z)sin\frac{n\pi}{\Theta}\theta - \bar{\bar{v}}_n(r,z)cos\frac{n\pi}{\Theta}\theta\right] \\ w(r,z,\theta) &= \sum_{n=0}^{Nh}\left[\bar{w}_n(r,z)cos\frac{n\pi}{\Theta}\theta + \bar{\bar{w}}_n(r,z)sin\frac{n\pi}{\Theta}\theta\right] \\ \Phi(r,z,\theta) &= \sum_{n=0}^{Nh}\left[\bar{\Phi}_n(r,z)cos\frac{n\pi}{\Theta}\theta + \bar{\bar{\Phi}}_n(r,z)sin\frac{n\pi}{\Theta}\theta\right] \end{aligned} \quad (16)$$

where Θ is the revolution amplitude around the z axis of the structure. Nh is the number of harmonics ($Nh = 0, 1, 2, \dots \infty$) which is used to identify accuracy approximation for unknown dependent variables through the circumferential direction. $\bar{u}_n$, $\bar{v}_n$ and $\bar{w}_n$ present the ordinary parameters of mechanical displacement in r, θ and z directions, respectively. Also $\bar{\bar{u}}_n$,$\bar{\bar{v}}_n$ and $\bar{\bar{w}}_n$ are

nominated as the complementary terms of mechanical displacement. Based on this definition, $\bar{\Phi}_n$ and $\bar{\bar{\Phi}}_n$are the ordinary and complementary terms of electrical potentials, respectively. Nomination of this terms was based on the cylinder behavior when $Nh = 0$. We specified $\bar{u}_n$, $\bar{v}_n$, $\bar{w}_n$ and $\bar{\Phi}_n$ as ordinary parameters so that $\bar{u}_n$, $\bar{v}_n$ and $\bar{w}_n$ could represent the ordinary symmetric displacements in the torsional vibration mode of the cylinder without warping in the case of $Nh = 0$. Thus, $\bar{\bar{u}}_n, \bar{\bar{v}}_n, \bar{\bar{w}}_n$ and $\bar{\bar{\Phi}}_n$ as the counterpoint of $\bar{u}_n$, $\bar{v}_n$, $\bar{w}_n$ and $\bar{\Phi}_n$, are outlined as the complementary terms which specify the pure warping mode by considering $Nh = 0$. Furthermore, the minus sign in the expansion of the circumferential displacement causes that the ordinary and complementary modes become identical in the cases of $Nh \neq 0$. Another well-known characteristic of this expansion is that the bases of Fourier series are orthogonal and satisfy Eq. (17) which makes the ordinary and complementary modes independent as we can see in the next section.

$$\begin{gathered}\int_{-\Theta}^{\Theta} sin\frac{n\pi}{\Theta}\theta cos\frac{m\pi}{\Theta}\theta d\theta = 0, for\ all\ n,m = 0,1,2,\dots \\ \int_{-\Theta}^{\Theta} sin\frac{n\pi}{\Theta}\theta sin\frac{m\pi}{\Theta}\theta d\theta = \int_{-\Theta}^{\Theta} cos\frac{n\pi}{\Theta}\theta cos\frac{m\pi}{\Theta}\theta d\theta \\ = 0, for\ all\ n \neq m\end{gathered} \tag{17}$$

And the matrix form of Eq. (16) can be written as follows:

$$\begin{gathered}U(r,z,\theta) = \sum_{n=0}^{Nh}\left[\bar{\theta}_n\bar{U}_n(r,z) + \bar{\bar{\theta}}_n\bar{\bar{U}}_n(r,z)\right], \bar{U}_n(r,z) \\ = \begin{bmatrix}\bar{u}_n \\ \bar{v}_n \\ \bar{w}_n\end{bmatrix}, \bar{\bar{U}}_n(r,z) = \begin{bmatrix}\bar{\bar{u}}_n \\ \bar{\bar{v}}_n \\ \bar{\bar{w}}_n\end{bmatrix} \\ \bar{\theta}_n = \begin{bmatrix}cosn\theta & 0 & 0 \\ 0 & sinn\theta & 0 \\ 0 & 0 & cosn\theta\end{bmatrix}, \bar{\bar{\theta}}_n \\ = \begin{bmatrix}sinn\theta & 0 & 0 \\ 0 & -cosn\theta & 0 \\ 0 & 0 & sinn\theta\end{bmatrix}\end{gathered} \tag{18}$$

3.3 Moving least squares formulation

In this paper, a mesh-free method based on the moving least squares shape function is applied to approximate dependent variables with respect to radial and axial directions. The excellent description of the MLS shape function and its relevant details have been provided by Lancaster and Salkausdas (Lancaster and Salkauskas 1981); consequently, a summarized expression of the MLS shape function corresponding to our configuration is provided in the following sections. As the first step, it is assumed that the dependent variables at any arbitrary point,$Q = \begin{vmatrix}r \\ z\end{vmatrix}$, in the structure's domain, Ω, have a form as Eq. (19).

$$\begin{gathered}X = \sum_{i=1}^{m} P_i(r,z)a_i(r,z) = \boldsymbol{P}^T(r,z)\boldsymbol{a}(r,z), \boldsymbol{P} \\ = [p_1\ p_2\ \dots\ p_m]^T, \boldsymbol{a} = [a_1\ a_2\ \dots\ a_m]\end{gathered} \tag{19}$$

where $X(r,z)$ can be representative of any ordinary and complementary terms of Eq. (16) at arbitrary point Q. p_i and a_i $(i = 1,2,\dots m)$ are the basic functions of the MLS method as defined in Eq. (20) and unknown coefficients, and m is the number of basic functions. Unlike other types of mesh-free shape function, the unknown vector $\boldsymbol{a}$ is a function of r and z. In order to determine these coefficients, an equations system is constructed based on the value of X at the field nodes of the support domain which is a rectangular cell centered at Q. Field nodes are the scattered nodes in order to approximate the dependent variables. The equation system has no solution because the number of equations, which is equal to the number of field nodes in the support domain, is usually larger than the number of basic functions and unknown coefficients; thus, the equation system should be solved by minimizing a residual function so called weighted discrete L_2-norm and is expressed as Eq. (21).

$$\boldsymbol{P}(r,z) = [1\ \ r\ \ z\ ]^T \tag{20}$$

$$J = \sum_{i=1}^{n} W_i(r,z)\left[\boldsymbol{P}^T(r_i,z_i)\boldsymbol{a}(r,z) - X(r_i,z_i)\right]^2 \tag{21}$$

where W_i is the relative weight function which is calculated based on the location of the arbitrary point $(Q = (r,z))$ and the location of the i_{th} field node (r_i,z_i) of the corresponding support domain. n is considered as the number of field nodes in the support domain centered at arbitrary point Q. It should be mentioned that the smoothness of the nodal shape function completely depends on the type of weight function. In the present work, the usual fourth-order spline weight function is selected as Eq. (22).

$$\begin{gathered}W_i(\bar{r}) = \begin{cases}1 - 6\bar{r}_i^2 + 8\bar{r}_i^3 - 3\bar{r}_i^4 & \bar{r}_i \leq 1 \\ 0 & \bar{r}_i > 1\end{cases} \\ W_i(\bar{z}) = \begin{cases}1 - 6\bar{z}_i^2 + 8\bar{z}_i^3 - 3\bar{z}_i^4 & \bar{z}_i \leq 1 \\ 0 & \bar{z}_i > 1\end{cases} \\ W_i(r,z) = W_i(\bar{r})W_i(\bar{z}) \\ \bar{r} = \frac{\|r - r_i\|}{ds} \\ \bar{z} = \frac{\|z - z_i\|}{ds}\end{gathered} \tag{22}$$

where ds is the size of the support domain and calculated as follow:

$$ds = dc * \alpha \tag{23}$$

dc is the average distance of between the field nodes, and α is the dimensionless size of support domain that $\alpha = 2.0{\sim}3.0$ leads to gain satisfying results. It should be noted that the approximation function, $X(r,z)$, may not pass through the real value. Thus, values of the $X(r_i,z_i)$ in Eq. (21) are not real and demonstrated by $\hat{X}(r,z)$. Finally, by minimizing a weighted discrete L_2 -norm, the coefficients vector a can be obtained as Eq. (24).

$$\boldsymbol{a}(r,z) = [A(r,z)]^{-1}B(r,z)\,\hat{\boldsymbol{X}} \tag{24}$$

where $\hat{\boldsymbol{X}}$ is $[\hat{x}(r_1,z_1)\ \hat{\boldsymbol{x}}(r_2,z_2)\ \dots\ \hat{\boldsymbol{x}}(r_n,z_n)]^T$. The moment

matrix $A(r,z)$ and matrix $B(r,z)$ are described as follows:

$$A(r,z)=\sum_{i=1}^{n} W_i(r,z)P(r_i,z_i)P^T(r_i,z_i)$$
$$B(r,z)_{(1,i)}=W_i(r,z)P(r_i,z_i) \tag{25}$$

Using equation (24) in equation (19) leads to:

$$X(r,z)=\boldsymbol{P}^T(r,z)[A(r,z)]^{-1}B(r,z)\,\hat{\boldsymbol{X}} \tag{26}$$

The Eq. (26) can be rewritten as $X(r,z)=\sum_{i=1}^{n}\psi_i(r,z)\hat{X}(r_i,z_i)$ or $X(r,z)=\Psi^T\hat{X}$, where ψ_i is known as the i_{th} shape functions corresponding to the i_{th} node in the support domain and $\Psi^T=[\psi_1(r,z)\ \psi_2(r,z)\ \dots\ \psi_n(r,z)]$ which are defined as follow:

$$\begin{aligned}\psi_i(r,z)&=\boldsymbol{P}^T(r,z)\big([A(r,z)]^{-1}B(r,z)\big)_i,\\ \Psi^T&=\boldsymbol{P}^T(r,z)[A(r,z)]^{-1}B(r,z)\end{aligned} \tag{27}$$

Index i shows the i_{th} column of the matrix$[A(r,z)]^{-1}B(r,z)$. As it is mentioned, $X(r,z)$ is representative of any ordinary and complementary terms of Eq. (16) at arbitrary point Q, so the MLS method allows us to approximate as follows:

$$\begin{aligned}
\bar{u}_n(r,z)&=\sum_{i=1}^{n}\psi_i(r,z)\hat{u}_n^i,\ \hat{u}_n^i=\hat{u}_n(r_i,z_i)\\
\bar{\bar{u}}_n(r,z)&=\sum_{i=1}^{n}\psi_i(r,z)\hat{\bar{u}}_n^i,\ \hat{\bar{u}}_n^i=\hat{\bar{u}}_n(r_i,z_i)\\
\bar{v}_n(r,z)&=\sum_{i=1}^{n}\psi_i(r,z)\hat{v}_n^i,\ \hat{v}_n^i=\hat{v}_n(r_i,z_i)\\
\bar{\bar{v}}_n(r,z)&=\sum_{i=1}^{n}\psi_i(r,z)\hat{\bar{v}}_n^i,\ \hat{\bar{v}}_n^i=\hat{\bar{v}}_n(r_i,z_i)\\
\bar{w}_n(r,z)&=\sum_{i=1}^{n}\psi_i(r,z)\hat{w}_n^i,\ \hat{w}_n^i=\hat{w}_n(r_i,z_i)\\
\bar{\bar{w}}_n(r,z)&=\sum_{i=1}^{n}\psi_i(r,z)\hat{\bar{w}}_n^i,\ \hat{\bar{w}}_n^i=\hat{\bar{w}}_n(r_i,z_i)\\
\bar{\Phi}_n(r,z)&=\sum_{i=1}^{n}\psi_i(r,z)\hat{\phi}_n^i,\ \hat{\phi}_n^i=\hat{\Phi}_n(r_i,z_i)\\
\bar{\bar{\Phi}}_n(r,z)&=\sum_{i=1}^{n}\psi_i(r,z)\hat{\bar{\phi}}_n^i,\ \hat{\bar{\phi}}_n^i=\hat{\bar{\Phi}}_n(r_i,z_i)
\end{aligned} \tag{28}$$

It is better to represent the Eq. (28) in the matrix form as follows:

$$\begin{aligned}
\bar{U}_{nh}(r,z)&=N_U\hat{\boldsymbol{q}}_{nh},\hat{\boldsymbol{q}}_{nh}=[\hat{q}_{nh}^1\ \hat{q}_{nh}^2\ \dots\ \hat{q}_{nh}^n]^T,\\
\hat{q}_{nh}^i&=\left[\hat{u}_{nh}^i\ \hat{v}_{nh}^i\ \hat{w}_{nh}^i\right]^T\\
\bar{\bar{U}}_{nh}(r,z)&=N_U\hat{\bar{\boldsymbol{q}}}_{nh},\hat{\bar{\boldsymbol{q}}}_{nh}=\left[\hat{\bar{q}}_{nh}^1\ \hat{\bar{q}}_{nh}^2\ \dots\ \hat{\bar{q}}_{nh}^n\right]^T\\
\hat{\bar{q}}_{nh}^i&=\left[\hat{\bar{u}}_{nh}^i\ \hat{\bar{v}}_{nh}^i\ \hat{\bar{w}}_{nh}^i\right]^T\\
\bar{\Phi}_{nh}(r,z)&=N_\Phi\hat{\boldsymbol{\phi}}_{nh},\hat{\boldsymbol{\phi}}_{nh}=\left[\hat{\phi}_{nh}^1\ \hat{\phi}_{nh}^2\ \dots\ \hat{\phi}_{nh}^n\right]^T\\
\bar{\bar{\Phi}}_{nh}(r,z)&=N_\Phi\hat{\bar{\boldsymbol{\phi}}}_{nh},\hat{\bar{\boldsymbol{\phi}}}_{nh}=\left[\hat{\bar{\phi}}_{nh}^1\ \hat{\bar{\phi}}_{nh}^2\ \dots\ \hat{\bar{\phi}}_{nh}^n\right]^T
\end{aligned} \tag{29}$$

where $N_U(\mathrm{r},\mathrm{z})$ and $N_\Phi(\mathrm{r},\mathrm{z})$ are the mechanical and electric shape function matrices which depend on location of either the arbitrary points and the field nodes of corresponding support domain and defined as below:

$$N_U(r,z)_{(i,3(n-1)+i)}=\psi_n(r,z),i=1,2,3 \tag{30}$$

$$N_\Phi(r,z)=[\psi_1(r,z)\quad\psi_2(r,z)\quad\dots\quad\psi_n(r,z)] \tag{31}$$

Also, the matrix form of Eq. (30) is shown in appendix F. As it can be seen in Eq. (12) and (15), it is necessary to determine the derivative of dependent variables and so the shape functions. Thus, the derivative of the shape functions can be obtained as follows. It should be noticed that the shape function has no derivative with respect to circumferential direction. To simplify obtaining the derivatives of shape function, Eq. (29) can be rewritten as $\Psi^T=\gamma^T B$ where $\gamma^T=\boldsymbol{P}^T A^{-1}$. The partial derivatives of shape function with respect to radial and axial coordinates can be calculated as follows:

$$\begin{aligned}
\Psi^T{}_{,r}&=\left(P_{,r}^T-\gamma^T A_{,r}\right)A^{-1}B+\gamma^T B_{,r}(r,z)\\
\Psi^T{}_{,z}&=\left(P_{,z}^T-\gamma^T A_{,z}\right)A^{-1}B+\gamma^T B_{,z}(r,z)
\end{aligned} \tag{32}$$

By substituting Eq. (16) and (28) in Eq. (3), the Hamilton principle involves integration evaluations. To obtain these integrations, the integral domain Ω divided into subdomains called background cells. So the integration can be calculated as the sum of integrations on the subdomains which they are obtained by Gaussian quadrature integration. Each background cell includes some Gauss points (nine Gauss points in this paper) to evaluate these integrations. Therefore, each Gauss point is considered as the arbitrary point Q which is mentioned in previous section. Dependent variables, shape functions and their derivatives are calculated at the location of these points. The terms of Hamilton principle can be rewritten by substituting Eq. (18) and (29) in Eq. (4), Eq. (5-a), (5-b) as follows:

$$\begin{aligned}
KE=-\int_{t_1}^{t_2}\sum_{i=1}^{NG}\int\Bigg[\Bigg(&\sum_{n=0}^{Nh}\delta\big(\bar{\theta}_n N_U\hat{\bar{q}}_n\\
&+\bar{\bar{\theta}}_n N_U\hat{\bar{\bar{q}}}_n\big)^T\Bigg)\rho\Bigg(\sum_{n=0}^{Nh}\frac{\partial^2}{\partial t^2}\big(\bar{\theta}_n N_U\hat{\bar{q}}_n\\
&+\bar{\bar{\theta}}_n N_U\hat{\bar{\bar{q}}}_n\big)\Bigg)\Bigg]d\Omega_i\ dt
\end{aligned} \tag{33}$$

$$\begin{aligned}
\rightarrow\int_{t_1}^{t_2}\delta KE\,dt=-\sum_{i=1}^{NG}\sum_{n=0}^{Nh}\Big[&\big(\delta\hat{\bar{q}}_n\big)^T\widehat{KE}_{1n}^{UU}\hat{\bar{\bar{q}}}_n\\
&+\big(\delta\hat{\bar{q}}_n\big)^T\widehat{KE}_{2n}^{UU}\hat{\bar{\bar{q}}}_n+\big(\delta\hat{\bar{\bar{q}}}_n\big)^T\widehat{KE}_{3n}^{UU}\hat{\bar{\bar{q}}}_n\\
&+\big(\delta\hat{\bar{\bar{q}}}_n\big)^T\widehat{KE}_{4n}^{UU}\hat{\bar{\bar{q}}}_n\Big]
\end{aligned}$$

where $\widehat{KE}_{1n}^{UU}$, $\widehat{KE}_{2n}^{UU}$, $\widehat{KE}_{3n}^{UU}$ and $\widehat{KE}_{4n}^{UU}$ are defined in

appendix A, and NG is considered as the number background cells in the support domain and also each term of the enthalpy is rewritten as bellow:

$$H=\sum_{i=1}^{NG}\int\left(\frac{1}{2}S^{T}T-\frac{1}{2}E^{T}D\right)d\Omega_{i}$$
$$\rightarrow\delta H=\sum_{i=1}^{NG}\int(\delta S^{T}C^{E}S-\delta S^{T}e^{T}E-\delta S^{T}C^{E}\alpha\Delta T-\delta E^{T}eS-\delta E^{T}\xi E-\delta E^{T}p\Delta T)d\Omega_{i} \tag{34}$$

By substituting Eq. (29) and (16) in former equation, the six terms of enthalpy can be described which are available in the Appendix B section. By simplifying these six terms, the final form of enthalpy equation is presented in the Appendix D.

The work done by external forces is described in Appendix C.

By substituting obtaining terms of kinetic energy, enthalpy and work done by external forces in Hamilton principle, and by considering coefficients of the $\delta\hat{\bar{q}}_n^T$ ،$\delta\hat{\bar{\bar{q}}}_n^T$ ، $\delta\hat{\bar{\phi}}_n^T$, $\delta\hat{\bar{\bar{\phi}}}_n^T$ terms as zero, the matrix form of govern equation is drawn as bellow:

$$\begin{bmatrix}\hat{T}_{1n}^{UU} & \hat{T}_{2n}^{UU} & 0 & 0\\ \hat{T}_{3n}^{UU} & \hat{T}_{4n}^{UU} & 0 & 0\\ 0 & 0 & 0 & 0\\ 0 & 0 & 0 & 0\end{bmatrix}\begin{bmatrix}\hat{\bar{\bar{q}}}_n\\ \hat{\bar{\bar{q}}}_n\\ \hat{\bar{\bar{\phi}}}_n\\ \hat{\bar{\bar{\phi}}}_n\end{bmatrix}$$
$$+\begin{bmatrix}\hat{H}_{1n}^{UU}-\hat{H}_{1n}^{U\Delta T} & \hat{H}_{2n}^{UU}-\hat{H}_{2n}^{U\Delta T} & \hat{H}_{1n}^{U\Phi} & \hat{H}_{2n}^{U\Phi}\\ \hat{H}_{3n}^{UU}-\hat{H}_{3n}^{U\Delta T} & \hat{H}_{4n}^{UU}-\hat{H}_{4n}^{U\Delta T} & \hat{H}_{3n}^{U\Phi} & \hat{H}_{4n}^{U\Phi}\\ \hat{H}_{1n}^{\Phi U} & \hat{H}_{2n}^{\Phi U} & -\hat{H}_{1n}^{\Phi\Phi} & -\hat{H}_{2n}^{\Phi\Phi}\\ \hat{H}_{3n}^{\Phi U} & \hat{H}_{4n}^{\Phi U} & -\hat{H}_{3n}^{\Phi\Phi} & -\hat{H}_{4n}^{\Phi\Phi}\end{bmatrix}\begin{bmatrix}\hat{\bar{q}}_n\\ \hat{\bar{\bar{q}}}_n\\ \hat{\bar{\phi}}_n\\ \hat{\bar{\bar{\phi}}}_n\end{bmatrix} \tag{35}$$
$$=\begin{bmatrix}\hat{F}_{1n}^{\Delta T}+\hat{F}_{1}^{b}+\hat{F}_{1}^{s}\\ \hat{F}_{2n}^{\Delta T}+\hat{F}_{2}^{b}+\hat{F}_{2}^{s}\\ -\hat{Q}_{1n}^{\Delta T}+\hat{Q}_{1}^{b}+\hat{Q}_{1}^{s}\\ -\hat{Q}_{2n}^{\Delta T}+\hat{Q}_{2}^{b}+\hat{Q}_{2}^{s}\end{bmatrix}$$

where

$$\bar{q}_{in}=\int_{-\Theta}^{\Theta}\bar{\theta}_n\begin{bmatrix}u_i\\ v_i\\ w_i\end{bmatrix}d\theta\,,\bar{\bar{q}}_{in}=\int_{-\Theta}^{\Theta}\bar{\bar{\theta}}_n\begin{bmatrix}u_i\\ v_i\\ w_i\end{bmatrix}d\theta$$
$$\bar{\Phi}_n=\int_{-\Theta}^{\Theta}cosn\theta\phi d\theta\,,\bar{\bar{\Phi}}_n=\int_{-\Theta}^{\Theta}sinn\theta\phi d\theta \tag{36}$$

The global form of the final equation (35) is written as Eq. (37).

$$\hat{M}_n^G\ddot{X}+\hat{K}_n^GX=\hat{F}_n^G,X=\left[\hat{\boldsymbol{q}}\;\hat{\boldsymbol{\phi}}\right]^T \tag{37}$$

By separating Eq. (35) corresponding to terms of displacement and electric potential fields, the final matrix form of govern equation is obtained as follows:

$$\begin{bmatrix}\hat{M}_{1n}^{UU} & \hat{M}_{2n}^{UU}\\ \hat{M}_{3n}^{UU} & \hat{M}_{4n}^{UU}\end{bmatrix}\begin{bmatrix}\hat{\bar{\bar{q}}}_n\\ \hat{\bar{\bar{q}}}_n\end{bmatrix}+\begin{bmatrix}\hat{K}_{1n}^{UU} & \hat{K}_{2n}^{UU}\\ \hat{K}_{3n}^{UU} & \hat{K}_{4n}^{UU}\end{bmatrix}\begin{bmatrix}\widehat{\bar{q}_n}\\ \widehat{\bar{\bar{q}}_n}\end{bmatrix}$$
$$+\begin{bmatrix}\hat{K}_{1n}^{U\Phi} & \hat{K}_{2n}^{U\Phi}\\ \hat{K}_{3n}^{U\Phi} & \hat{K}_{4n}^{U\Phi}\end{bmatrix}\begin{bmatrix}\widehat{\bar{\phi}_n}\\ \widehat{\bar{\bar{\phi}}_n}\end{bmatrix}=\begin{bmatrix}\hat{F}_{1n}\\ \hat{F}_{2n}\end{bmatrix} \tag{38-a}$$

$$\begin{bmatrix}\hat{K}_{1n}^{\Phi U} & \hat{K}_{2n}^{\Phi U}\\ \hat{K}_{3n}^{\Phi U} & \hat{K}_{4n}^{\Phi U}\end{bmatrix}\begin{bmatrix}\widehat{\bar{q}_n}\\ \widehat{\bar{\bar{q}}_n}\end{bmatrix}-\begin{bmatrix}\hat{K}_{1n}^{\Phi\Phi} & \hat{K}_{2n}^{\Phi\Phi}\\ \hat{K}_{3n}^{\Phi\Phi} & \hat{K}_{4n}^{\Phi\Phi}\end{bmatrix}\begin{bmatrix}\widehat{\bar{\phi}_n}\\ \widehat{\bar{\bar{\phi}}_n}\end{bmatrix}=\begin{bmatrix}\hat{Q}_{1n}\\ \hat{Q}_{2n}\end{bmatrix} \tag{38-b}$$

Where

$$\begin{bmatrix}\hat{M}_{1n}^{UU} & \hat{M}_{2n}^{UU}\\ \hat{M}_{3n}^{UU} & \hat{M}_{4n}^{UU}\end{bmatrix}=\begin{bmatrix}\hat{T}_{1n}^{UU} & \hat{T}_{2n}^{UU}\\ \hat{T}_{3n}^{UU} & \hat{T}_{4n}^{UU}\end{bmatrix}$$
$$\begin{bmatrix}\hat{K}_{1n}^{UU} & \hat{K}_{2n}^{UU}\\ \hat{K}_{3n}^{UU} & \hat{K}_{4n}^{UU}\end{bmatrix}=\begin{bmatrix}\hat{H}_{1n}^{UU}-\hat{H}_{1n}^{U\Delta T} & \hat{H}_{2n}^{UU}-\hat{H}_{2n}^{U\Delta T}\\ \hat{H}_{3n}^{UU}-\hat{H}_{3n}^{U\Delta T} & \hat{H}_{4n}^{UU}-\hat{H}_{4n}^{U\Delta T}\end{bmatrix}$$
$$\begin{bmatrix}\hat{K}_{1n}^{U\Phi} & \hat{K}_{2n}^{U\Phi}\\ \hat{K}_{3n}^{U\Phi} & \hat{K}_{4n}^{U\Phi}\end{bmatrix}=\begin{bmatrix}\hat{H}_{1n}^{U\Phi} & \hat{H}_{2n}^{U\Phi}\\ \hat{H}_{3n}^{U\Phi} & \hat{H}_{4n}^{U\Phi}\end{bmatrix}$$
$$\begin{bmatrix}\hat{K}_{1n}^{\Phi U} & \hat{K}_{2n}^{\Phi U}\\ \hat{K}_{3n}^{\Phi U} & \hat{K}_{4n}^{\Phi U}\end{bmatrix}=\begin{bmatrix}\hat{H}_{1n}^{\Phi U} & \hat{H}_{2n}^{\Phi U}\\ \hat{H}_{3n}^{\Phi U} & \hat{H}_{4n}^{\Phi U}\end{bmatrix} \tag{39}$$
$$\begin{bmatrix}\hat{K}_{1n}^{\Phi\Phi} & \hat{K}_{2n}^{\Phi\Phi}\\ \hat{K}_{3n}^{\Phi\Phi} & \hat{K}_{4n}^{\Phi\Phi}\end{bmatrix}=\begin{bmatrix}\hat{H}_{1n}^{\Phi\Phi} & \hat{H}_{2n}^{\Phi\Phi}\\ \hat{H}_{3n}^{\Phi\Phi} & \hat{H}_{4n}^{\Phi\Phi}\end{bmatrix}$$
$$\begin{bmatrix}\hat{F}_{1n}\\ \hat{F}_{2n}\end{bmatrix}=\begin{bmatrix}\hat{F}_{1n}^{\Delta T}+\hat{F}_{1}^{b}+\hat{F}_{1}^{s}\\ \hat{F}_{2n}^{\Delta T}+\hat{F}_{2}^{b}+\hat{F}_{2}^{s}\end{bmatrix}$$
$$\begin{bmatrix}\hat{Q}_{1n}\\ \hat{Q}_{2n}\end{bmatrix}=\begin{bmatrix}-\hat{Q}_{1n}^{\Delta T}+\hat{Q}_{1}^{b}+\hat{Q}_{1}^{s}\\ -\hat{Q}_{2n}^{\Delta T}+\hat{Q}_{2}^{b}+\hat{Q}_{2}^{s}\end{bmatrix}$$

And each component of former equation is calculated in the Appendix D. For solving Eq. (38-a), it is required to obtain $\begin{bmatrix}\widehat{\bar{\phi}_n}\\ \widehat{\bar{\bar{\phi}}_n}\end{bmatrix}$ from Eq. (38-b) as follows:

$$\begin{bmatrix}\widehat{\bar{\phi}_n}\\ \widehat{\bar{\bar{\phi}}_n}\end{bmatrix}=\begin{bmatrix}\hat{K}_{1n}^{\Phi\Phi} & \hat{K}_{2n}^{\Phi\Phi}\\ \hat{K}_{3n}^{\Phi\Phi} & \hat{K}_{4n}^{\Phi\Phi}\end{bmatrix}^{-1}\left(\begin{bmatrix}\hat{K}_{1n}^{\Phi U} & \hat{K}_{2n}^{\Phi U}\\ \hat{K}_{3n}^{\Phi U} & \hat{K}_{4n}^{\Phi U}\end{bmatrix}\begin{bmatrix}\widehat{\bar{q}_n}\\ \widehat{\bar{\bar{q}}_n}\end{bmatrix}-\begin{bmatrix}\hat{Q}_{1n}\\ \hat{Q}_{2n}\end{bmatrix}\right) \tag{40}$$

Then by substituting the Eq. (40) in (38-a), $\begin{bmatrix}\widehat{\bar{q}_n}\\ \widehat{\bar{\bar{q}}_n}\end{bmatrix}$ can be evaluated as bellow:

$$\begin{bmatrix}\hat{M}_{1n}^{UU} & \hat{M}_{2n}^{UU}\\ \hat{M}_{3n}^{UU} & \hat{M}_{4n}^{UU}\end{bmatrix}\begin{bmatrix}\hat{\bar{\bar{q}}}_n\\ \hat{\bar{\bar{q}}}_n\end{bmatrix}$$
$$+\left(\begin{bmatrix}\hat{K}_{1n}^{UU} & \hat{K}_{2n}^{UU}\\ \hat{K}_{3n}^{UU} & \hat{K}_{4n}^{UU}\end{bmatrix}\right.$$
$$\left.+\begin{bmatrix}\hat{K}_{1n}^{U\Phi} & \hat{K}_{2n}^{U\Phi}\\ \hat{K}_{3n}^{U\Phi} & \hat{K}_{4n}^{U\Phi}\end{bmatrix}\begin{bmatrix}\hat{K}_{1n}^{\Phi\Phi} & \hat{K}_{2n}^{\Phi\Phi}\\ \hat{K}_{3n}^{\Phi\Phi} & \hat{K}_{4n}^{\Phi\Phi}\end{bmatrix}^{-1}\begin{bmatrix}\hat{K}_{1n}^{\Phi U} & \hat{K}_{2n}^{\Phi U}\\ \hat{K}_{3n}^{\Phi U} & \hat{K}_{4n}^{\Phi U}\end{bmatrix}\right)\begin{bmatrix}\widehat{\bar{q}_n}\\ \widehat{\bar{\bar{q}}_n}\end{bmatrix} \tag{41}$$
$$=\begin{bmatrix}\hat{F}_{1n}\\ \hat{F}_{2n}\end{bmatrix}+\begin{bmatrix}\hat{K}_{1n}^{\Phi\Phi} & \hat{K}_{2n}^{\Phi\Phi}\\ \hat{K}_{3n}^{\Phi\Phi} & \hat{K}_{4n}^{\Phi\Phi}\end{bmatrix}^{-1}\begin{bmatrix}\hat{Q}_{1n}\\ \hat{Q}_{2n}\end{bmatrix}$$

For free vibration analysis, the body and surface force terms in Eq. (41) should be neglected as Eq. (42).

$$\begin{bmatrix}\hat{M}_{1n}^{UU} & \hat{M}_{2n}^{UU}\\ \hat{M}_{3n}^{UU} & \hat{M}_{4n}^{UU}\end{bmatrix}\begin{bmatrix}\hat{\bar{\bar{q}}}_n\\ \hat{\bar{\bar{q}}}_n\end{bmatrix}$$
$$+\left(\begin{bmatrix}\hat{K}_{1n}^{UU} & \hat{K}_{2n}^{UU}\\ \hat{K}_{3n}^{UU} & \hat{K}_{4n}^{UU}\end{bmatrix}\right. \tag{42}$$
$$\left.+\begin{bmatrix}\hat{K}_{1n}^{U\Phi} & \hat{K}_{2n}^{U\Phi}\\ \hat{K}_{3n}^{U\Phi} & \hat{K}_{4n}^{U\Phi}\end{bmatrix}\begin{bmatrix}\hat{K}_{1n}^{\Phi\Phi} & \hat{K}_{2n}^{\Phi\Phi}\\ \hat{K}_{3n}^{\Phi\Phi} & \hat{K}_{4n}^{\Phi\Phi}\end{bmatrix}^{-1}\begin{bmatrix}\hat{K}_{1n}^{\Phi U} & \hat{K}_{2n}^{\Phi U}\\ \hat{K}_{3n}^{\Phi U} & \hat{K}_{4n}^{\Phi U}\end{bmatrix}\right)\begin{bmatrix}\widehat{\bar{q}_n}\\ \widehat{\bar{\bar{q}}_n}\end{bmatrix}=0$$

3.4 Transformation matrix

As it is said, owing to the number of nodes in the corresponding support domain is usually larger than the

number of components of basic function, the curve of shape function does not pass through all nodal values; thus, it is incorrect to enforce essential boundary conditions directly. Based on this reason, the values of $\hat{\bar{q}}$, $\hat{\bar{\bar{q}}}$, $\hat{\bar{\Phi}}$ and $\hat{\bar{\bar{\Phi}}}$ should be modified. In this paper, the transformation matrix method is employed to turn the fictitious values of mechanical displacements and electric potentials to actual values to makes it possible to impose essential boundary conditions (Atluri, Kim *et al*. 1999; Foroutan, Mohammadi *et al*. 2017). The structures of these transformation matrices are described, as is shown in appendix E. Where T_u and T_Φ are transformation matrices related to mechanical displacements and electrical potentials, respectively. $\psi_i(\mathrm{r}_j, \mathrm{z}_j)$ is i_{th} shape function related to the j_{th} field node as the center of support domain. The actual values of ordinary and complementary field variables can be evaluated as Eq. (43) (Foroutan, Mohammadi *et al*. 2017).

$$\begin{aligned} \bar{q} &= T_u \hat{\bar{q}} \\ \bar{\bar{q}} &= T_u \hat{\bar{\bar{q}}} \\ \bar{\Phi} &= T_\Phi \hat{\bar{\Phi}} \\ \bar{\bar{\Phi}} &= T_\Phi \hat{\bar{\bar{\Phi}}} \end{aligned} \tag{43}$$

In which $\bar{q}$ and $\bar{\bar{q}}$ are the actual values of ordinary and complimentary total displacement vector. Also, $\bar{\Phi}$ and $\bar{\bar{\Phi}}$ are the actual values of ordinary and complimentary total potential vector. By substituting Eq. (43) in every term of Hamilton principle, Eq. (42) can be rearranged as bellow:

$$\begin{aligned} &\begin{bmatrix} M_{1n}^{UU} & M_{2n}^{UU} \\ M_{3n}^{UU} & M_{4n}^{UU} \end{bmatrix} \begin{bmatrix} \ddot{\bar{q}}_n \\ \ddot{\bar{\bar{q}}}_n \end{bmatrix} \\ &+ \left(\begin{bmatrix} K_{1n}^{UU} & K_{2n}^{UU} \\ K_{3n}^{UU} & K_{4n}^{UU} \end{bmatrix} \right. \\ &\left. + \begin{bmatrix} K_{1n}^{U\Phi} & K_{2n}^{U\Phi} \\ K_{3n}^{U\Phi} & K_{4n}^{U\Phi} \end{bmatrix} \begin{bmatrix} K_{1n}^{\Phi\Phi} & K_{2n}^{\Phi\Phi} \\ K_{3n}^{\Phi\Phi} & K_{4n}^{\Phi\Phi} \end{bmatrix}^{-1} \begin{bmatrix} K_{1n}^{\Phi U} & K_{2n}^{\Phi U} \\ K_{3n}^{\Phi U} & K_{4n}^{\Phi U} \end{bmatrix} \right) \begin{bmatrix} \bar{q}_n \\ \bar{\bar{q}}_n \end{bmatrix} = 0 \end{aligned} \tag{44}$$

where

$$\begin{aligned} M_{in}^{UU} &= (T_u^{-1})^T \hat{M}_{in}^{UU} T_u^{-1} \\ K_{in}^{UU} &= (T_u^{-1})^T \hat{K}_{in}^{UU} T_u^{-1} \\ K_{in}^{U\Phi} &= (T_u^{-1})^T \hat{K}_{in}^{U\Phi} T_\Phi^{-1} \\ K_{in}^{\Phi U} &= (T_\Phi^{-1})^T \hat{K}_{in}^{\Phi U} T_u^{-1} \\ K_{in}^{\Phi\Phi} &= (T_\Phi^{-1})^T \hat{K}_{in}^{\Phi\Phi} T_\Phi^{-1} \end{aligned} \tag{45}$$

4. Results and discussion

4.1 Validation study

The authenticity of this paper was assessed by available work done by Jodaei *et al*. (Jodaei, Jalal *et al*. 2013). By employing state-space based differential quadrature (SSDQM) method, they obtained the first three non-dimensional natural frequency of axial directional FGP annular plate (inner radius=0.15m, outer radius=1.0m and L=0.1m, $\bar{\omega} = \omega L\sqrt{\rho_{PZT4}/C11_{PZT4}}$) with the clamped-clamped boundary (C-C) as mechanical boundary condition at inner and outer radius and the closed circuit as the electrical boundary condition at upper and lower surface as bellow:

$$u_r = u_z = u_\theta = 0 \text{ at } r = a, b; \ \varphi = 0 \ at \ z = 0, L. \tag{46}$$

They assumed the material properties vary through axial direction by following exponential distributions.

$$k = k^0 e^{\lambda\left(\frac{z}{L}\right)} \tag{47}$$

where k denotes material properties at the desired spot(r, z), and k^0 is the primary properties at center of bottom plate ($r = 0, \ z = 0$) which they are considered equal to the properties of PZT-4. λ denotes the material property axially graded index. By considering mentioned assumptions, the validation and convergence studies of the ordinary term of zeroth harmonic, first and second harmonic natural frequencies of the annular plate for different node distributions are presented in Table 1. The abbreviation for Or, Cmp mean ordinary and complementary terms of zeroth harmonic natural frequencies, and the abbreviation of F.H and S.H mean first harmonic and second harmonic terms of natural frequencies respectively. It clearly illustrates good agreement between the present results and those from Jodaei *et al*. (Jodaei, Jalal *et al*. 2013). It should be considered that they used different Fourier expansion and did not obtain the natural frequencies of pure warping mode of FGP cylinder, so there were no results for comparing this type of natural frequencies; thus, the complementary terms of zeroth harmonic natural frequencies are not mentioned in Table 1. Since the values of ordinary terms of first and second harmonic natural frequencies are equal to the values complementary terms of first and second harmonic, it is just written first and second harmonic in all tables.

4.2 Radial polarized study

In this section, the effects of various parameters on the natural frequencies are carried out. It is assumed the structure has C-C boundary conditions at upper and lower surface as mechanical condition and close circuit at inner and outer surface as the electric boundary conditions. It is considered the structure has been made of PZT-4, PZT-5A, PZT-8 and PZT-5H by following the power law distribution as Eq. (1). Based on this power law, the lowest and highest point of the inner surface are rich PZT-4 and PZT-5A, respectively. Also, the lowest and highest point of the outer surface are rich PZT-8 and PZT-5H, respectively. The properties of these piezoelectric materials are presented in Table 2.

Table 3 and 4 show the effects of temperature variation and different geometry parameters on the first five non-dimensional natural frequencies related to zeroth harmonics and non-zeroth harmonics of the radially polarized FGP hollow cylinder. As it is expected, these results clearly show that the natural frequencies decrease with increasing temperature since in lower temperature conditions,

Table 1 the lowest non-dimensional natural frequencies related to the zero, first and second harmonics of FGP annular plates having C-C boundary conditions (a = 1 m, b = 0.15 m, L = 0.1 m)

λ	Number of node	*Or*	*F.H*	*S.H*
1	5*5	0.0705	0.0729	0.0881
	6*6	0.0698	0.0722	0.0870
	6*8	0.0692	0.0715	0.0857
	6*10	0.0690	0.0713	0.0853
	Ref	0.0684	0.0717	0.0878
2	5*5	0.0671	0.0693	0.0832
	6*6	0.0658	0.0680	0.0815
	6*8	0.0649	0.0670	0.0800
	6*10	0.0644	0.0665	0.0794
	Ref	0.0634	0.0664	0.0807
5	5*5	0.0527	0.0541	0.0632
	6*6	0.0496	0.0510	0.0596
	6*8	0.0472	0.0485	0.0568
	6*10	0.0457	0.0471	0.0554
	Ref	0.0454	0.0474	0.057
10	5*5	0.0418	0.0427	0.0474
	6*6	0.0364	0.0369	0.0407
	6*8	0.0314	0.0319	0.0356
	6*10	0.0284	0.0290	0.0331
	Ref	0.0273	0.0286	0.0344

the structure is stiffer than in the higher temperature conditions. However, temperature's change in this range has a small effect on natural frequencies; in addition, higher h/a leads to obtain higher values of natural frequencies because in this type of boundary condition, stiffness of hollow cylinder increase by increasing thickness in radial direction; nevertheless, the natural frequencies decrease by ascending L/a, for the cylinder become more flexible. However, the intensity of the geometry parameters effects are different for symmetric modes, pure warping modes and non-zeroth harmonic modes. Let's look the first frequency of ordinary and complementary mode of zeroth harmonic. At a constant L/a, by decreasing the thickness, the first frequency of symmetric modes become smaller by more severity than of pure warping modes. However, at constant h/a, by increasing the length of the cylinder, dropping of frequencies for pure warping modes is bigger than the frequencies of symmetric modes. When h/a=0.4, first frequency of symmetric mode is bigger than of pure warping mode, and when the L/a increased from 1 to 5, this difference become more. Probably, with decreasing L/a, the difference will may be smaller and first frequency of symmetric mode become smaller than of pure warping mode. In the cases of h/a<0.4 and L/a=1, first frequency of symmetric modes is smaller than of pure warping modes. When L/a increased from 1 to 5, first frequency of symmetric modes become bigger even than second mode. The intensity of these two opposite effects, in some geometry, will be bigger for symmetric mode than pure warping modes and in other cases will be smaller. It should

Table 2 Material properties of basic constituents of the structure

	PZT-4	PZT-5H	PZT-5A	PZT-8
Elastic moduli ($\boldsymbol{10^{11}Pa}$)				
$\boldsymbol{C_{11}}$	1.3900	1.2720	1.2035	1.4688
$\boldsymbol{C_{12}}$	0.7784	0.8021	0.7518	0.8109
$\boldsymbol{C_{13}}$	0.7428	0.8467	0.7509	0.8105
$\boldsymbol{C_{22}}$	1.3900	1.2720	1.2035	1.4688
$\boldsymbol{C_{33}}$	1.1541	1.1744	1.1087	1.3171
$\boldsymbol{C_{44}}$	0.2564	0.2299	0.2105	0.3135
$\boldsymbol{C_{55}}$	0.2564	0.2299	0.2105	0.3135
$\boldsymbol{C_{66}}$	0.3040	0.2347	0.2257	0.3289
Piezoelectric moduli ($\boldsymbol{C\,m^{-2}}$)				
$\boldsymbol{e_{11}}$	15.0804	23.2403	15.7835	13.9108
$\boldsymbol{e_{12}}$	-5.2028	-6.6228	-5.3512	-3.8754
$\boldsymbol{e_{13}}$	-5.2028	-6.6228	-5.3512	-3.8754
$\boldsymbol{e_{26}}$	12.7179	17.0345	12.2947	10.3448
$\boldsymbol{e_{35}}$	12.7179	17.0345	12.2947	10.3448
Dielectric moduli ($\boldsymbol{10^{-8}F\,m^{-1}}$)				
$\boldsymbol{\eta_{11}}$	0.5872	1.269	0.7319	0.4972
$\boldsymbol{\eta_{22}}$	0.6752	1.509	0.8137	0.8008
$\boldsymbol{\eta_{33}}$	0.6752	1.509	0.8137	0.8008
Thermal expansion coefficient($\boldsymbol{10^{-5}}$)				
$\boldsymbol{\alpha_{11}}$	0.2	0.6	0.6	0.2
$\boldsymbol{\alpha_{22}}$	0.2	2.33	2.33	0.2
$\boldsymbol{\alpha_{33}}$	0.2	2.33	2.33	0.2
Density ($\boldsymbol{Kg\,m^{-3}}$)	7500	7500	7750	7600

be noted that the growth rate of complementary term of zeroth harmonic frequencies is higher than the growth rate of ordinary terms of zeroth harmonic frequencies. Therefore, in upper modes, regardless of geometry parameters, frequencies of pure warping mode will be bigger than the frequencies of symmetric modes.

Comparison between the frequencies of first harmonic and second harmonic, generally it should be noted that except in shallow cylinder case (h/a=0.05) at lower modes, the second harmonic modes have bigger natural frequencies than first harmonic ones. By increasing L/a first frequency of first harmonic is more sensitive than first frequency of the second harmonic and by increasing h/a the first frequency of the second harmonic is more sensitive than the first frequency of the first harmonic. The growth rate of frequencies related to the second harmonic is more than growth rate of frequency related to the first harmonic.

Table 3 Ordinary and complementary terms of first five zeroth harmonic natural frequencies of radial polarized bi-directional FGP Hollow Cylinder with C-C boundary conditions and n_r=2, n_z=1

h/a	M	*T*= 25℃		*T*= 50℃		*T*= 75℃	
		Or	*Cmp*	*Or*	*Cmp*	*Or*	*Cmp*
0.05 *L/a* =1	Ω_1	0.0428	0.0667	0.0423	0.0666	0.0419	0.0664
	Ω_2	0.0514	0.1347	0.0503	0.1345	0.0492	0.1343
	Ω_3	0.0789	0.2053	0.0774	0.2050	0.0759	0.2046
	Ω_4	0.1153	0.2789	0.1148	0.2785	0.1141	0.2781
	Ω_5	0.1227	0.3569	0.1215	0.3564	0.1204	0.3558
0.25 *L/a*=1	Ω_1	0.3290	0.3341	0.3281	0.3335	0.3271	0.3328
	Ω_2	0.5546	0.6747	0.5534	0.6736	0.5523	0.6725
	Ω_3	0.6216	1.0273	0.6206	1.0257	0.6197	1.0241
	Ω_4	0.9386	1.3942	0.9364	1.3921	09342	1.3900
	Ω_5	1.1767	1.4964	1.1758	1.4941	1.1750	1.4918
0.4 *L/a*=1	Ω_1	0.6322	0.5365	0.6311	0.5354	0.6300	0.5343
	Ω_2	0.9367	1.0830	0.9359	1.0813	0.9350	1.0795
	Ω_3	1.0972	1.5887	1.0951	1.5864	1.0931	1.5842
	Ω_4	1.6947	1.6484	1.6918	1.6458	1.6890	1.6433
	Ω_5	1.7356	1.8517	1.7338	1.8493	1.7319	1.8469
0.05 *L/a* =5	Ω_1	0.0210	0.0135	0.0209	0.0134	0.0209	0.0133
	Ω_2	0.0343	0.0271	0.0341	0.0270	0.0338	0.0269
	Ω_3	0.0368	0.0408	0.0364	0.0407	0.0358	0.0406
	Ω_4	0.0379	0.0547	0.0373	0.0546	0.0367	0.0545
	Ω_5	0.0389	0.0689	0.0383	0.0688	0.0377	0.0687
0.25 *L/a*=5	Ω_1	0.1072	0.0678	0.1071	0.0671	0.1070	0.0663
	Ω_2	0.1885	0.1360	0.1881	0.1355	0.1877	0.1349
	Ω_3	0.2142	0.2049	0.2135	0.2044	0.2128	0.2038
	Ω_4	0.2277	0.2747	0.2269	0.2741	0.2261	0.2736
	Ω_5	0.2439	0.3459	0.2431	0.3453	0.2423	0.3446
0.4 *L/a*=5	Ω_1	0.1731	0.1089	0.1730	0.1075	0.1728	0.1062
	Ω_2	0.3170	0.2183	0.3165	0.2174	0.3160	0.2165
	Ω_3	0.3783	0.3289	0.3774	0.3280	0.3765	0.3271
	Ω_4	0.4118	0.4410	0.4109	0.4401	0.4099	0.4391
	Ω_5	0.4460	0.5553	0.4451	0.5542	0.4443	0.5532

Table 4 First five non-zero harmonic natural frequencies of radial polarized bi-directional FGP Hollow Cylinder with C-C boundary conditions and n_r=2, n_z=1

h/a	*M*	*T*= 25℃		*T*= 50℃		*T*= 75℃	
		F.H	*S.H*	*F.H*	*S.H*	*F.H*	*S.H*
0.05 *L/a* =1	Ω_1	0.0358	0.0284	0.0354	0.0278	0.0350	0.0272
	Ω_2	0.0510	0.0499	0.0498	0.0487	0.0487	0.0474
	Ω_3	0.0775	0.0791	0.0763	0.0776	0.0750	0.0760
	Ω_4	0.0825	0.1083	0.0821	0.1081	0.0818	0.1080
	Ω_5	0.1122	0.1112	0.1120	0.1110	0.1118	0.1109
0.25 *L/a*=1	Ω_1	0.2817	0.2810	0.2808	0.2798	0.2799	0.2787
	Ω_2	0.4362	0.5602	0.4354	0.5593	0.4346	0.5584
	Ω_3	0.5612	0.5838	0.5603	0.5829	0.5594	0.5821
	Ω_4	0.5861	0.5979	0.5847	0.5963	0.5834	0.5947
	Ω_5	0.7474	0.8641	0.7464	0.8630	0.7454	0.8620
0.4 *L/a*=1	Ω_1	0.5163	0.5547	0.5153	0.5534	0.5143	0.5521
	Ω_2	0.7464	0.9100	0.7451	0.9087	0.7438	0.9074
	Ω_3	0.9140	0.9701	0.9130	0.9687	0.9120	0.9673
	Ω_4	1.0579	1.1147	1.0559	1.1126	1.0539	1.1105
	Ω_5	1.2266	1.4091	1.2248	1.4072	1.2231	1.4054
0.05 *L/a* =5	Ω_1	0.0088	0.0051	0.0087	0.0044	0.0087	0.0037
	Ω_2	0.0172	0.0103	0.0171	0.0099	0.0170	0.0094
	Ω_3	0.0255	0.0163	0.0253	0.0158	0.0251	0.0154
	Ω_4	0.0298	0.0219	0.0297	0.0213	0.0296	0.0208
	Ω_5	0.0308	0.0266	0.0305	0.0259	0.0302	0.0252
0.25 *L/a*=5	Ω_1	0.0453	0.0649	0.0450	0.0636	0.0448	0.0622
	Ω_2	0.0902	0.0906	0.0897	0.0894	0.0893	0.0881
	Ω_3	0.1406	0.1291	0.1399	0.1279	0.1392	0.1265
	Ω_4	0.1602	0.1753	0.1599	0.1739	0.1597	0.1725
	Ω_5	0.1867	0.2269	0.1857	0.2254	0.1847	0.2239
0.4 *L/a*=5	Ω_1	0.0748	0.1741	0.0744	0.1728	0.0741	0.1714
	Ω_2	0.1516	0.2162	0.1509	0.2149	0.1502	0.2135
	Ω_3	0.2438	0.2835	0.2429	0.2821	0.2420	0.2807
	Ω_4	0.2735	0.3686	0.2731	0.3671	0.2726	0.3657
	Ω_5	0.3405	0.4593	0.3393	0.4584	0.3381	0.4574

4.3 Axial polarized study

Tables 5 and 6 indicate the first five zero and the non-zero harmonics of natural frequencies of axially polarized thin ring (L/a=0.2) and thin hollow cylinder (L/a=1) respectively. In these cases, the top and bottom surfaces of structure are clamped (at $z = 0$, $u_{r=0}$, $u_{z=0}$, $u_{\theta=0}$; at $z = L$, $u_{r=0}$, $u_{z=0}$, $u_{\theta=0}$). As it is expected, natural frequencies increase with increasing h/a, and also decrease with increasing L/a. By increasing h/a, the growth rate in complementary terms of zero harmonic natural frequencies of thin ring is higher than the growth rate in ordinary terms of zero harmonic natural frequencies; nevertheless, for L/a=1, the growth rate in ordinary terms is higher. The growth rate in the first and second harmonic natural frequencies of the axially polarized thin ring and thin hollow cylinder are almost the same. Also, natural

Table 5 First five zero harmonic natural frequencies of axial polarized bi-directional FGP thin ring and FGP thin hollow cylinder with C-C conditions (n_r=2, n_z=1)

h/a	M	*T*= 25℃		*T*= 50℃		*T*= 75℃	
		Or	*Cmp*	*Or*	*Cmp*	*Or*	*Cmp*
0.03 *L/a* =0.2	Ω_1	1.6779	1.2718	1.6759	1.2690	1.6738	1.2662
	Ω_2	1.7251	1.3930	1.7244	1.3909	1.7237	1.3889
	Ω_3	1.9382	1.4495	1.9368	1.4483	1.9355	1.4472
	Ω_4	2.1714	1.5014	2.1686	1.4998	2.1658	1.4982
	Ω_5	2.2592	1.6046	2.2572	1.6026	2.2552	1.6006
0.04 *L/a*=0.2	Ω_1	1.6874	1.2991	1.6857	1.2964	1.6839	1.2937
	Ω_2	1.7390	1.4228	1.7380	1.4211	1.7369	1.4194
	Ω_3	2.1037	1.4868	2.1023	1.4854	2.1008	1.4841
	Ω_4	2.3908	1.6030	2.3877	1.6010	2.3845	1.5991
	Ω_5	2.5708	1.7789	2.5692	1.7765	2.5676	1.7742
0.05 *L/a*=0.2	Ω_1	1.6938	1.3145	1.6921	1.3119	1.6906	1.3093
	Ω_2	1.7727	1.4427	1.7714	1.4413	1.7700	1.4399
	Ω_3	2.2957	1.5399	2.2942	1.5382	2.2927	1.5365
	Ω_4	2.5156	1.7255	2.5127	1.7233	2.5098	1.7210
	Ω_5	2.7400	1.9805	2.7364	1.9778	2.7328	1.9750
0.03 *L/a* =1	Ω_1	1.1764	0.7801	1.1748	0.7781	1.1732	0.7761
	Ω_2	1.3333	0.8869	1.3321	0.8867	1.3307	0.8864
	Ω_3	1.3397	1.3133	1.3390	1.3108	1.3385	1.3082
	Ω_4	1.5424	1.3421	1.5422	1.3397	1.5420	1.3373
	Ω_5	1.7276	1.3616	1.7258	1.3589	1.7239	1.3562
0.04 *L/a*=1	Ω_1	1.2892	0.8688	1.2873	0.8666	1.2854	0.8644
	Ω_2	1.4563	1.0034	1.4546	1.0031	1.4529	1.0028
	Ω_3	1.5106	1.3179	1.5103	1.3153	1.5101	1.3128
	Ω_4	1.6511	1.3523	1.6509	1.3500	1.6506	1.3477
	Ω_5	1.7361	1.3812	1.7344	1.3791	1.7327	1.3770
0.05 *L/a*=1	Ω_1	1.3820	0.9480	1.3798	0.9456	1.3776	0.9432
	Ω_2	1.5569	1.1138	1.5550	1.1134	1.5532	1.1131
	Ω_3	1.6033	1.3224	1.6030	1.3198	1.6026	1.3173
	Ω_4	1.7456	1.3618	1.7440	1.3596	1.7424	1.3573
	Ω_5	1.7662	1.3948	1.7659	1.3928	1.7656	1.3909

Table 6 first five non-zero natural frequencies of axial polarized bi-directional FGP thin ring and FGP thin hollow cylinder with C-C boundary conditions (n_r=2, n_z=1)

h/a	M	T= 25℃		T= 50℃		T= 75℃	
		F.H	*S.H*	*F.H*	*S.H*	*F.H*	*S.H*
0.03 *L/a* =0.2	Ω_1	1.2720	1.2727	1.2692	1.2699	1.2664	1.2671
	Ω_2	1.3932	1.3939	1.3912	1.3919	1.3891	1.3898
	Ω_3	1.4497	1.4504	1.4485	1.4492	1.4474	1.4481
	Ω_4	1.5016	1.5021	1.5000	1.5005	1.4984	1.4989
	Ω_5	1.6047	1.6051	1.6028	1.6032	1.6008	1.6012
0.04 *L/a*=0.2	Ω_1	1.2995	1.3007	1.2968	1.2981	1.2942	1.2954
	Ω_2	1.4232	1.4244	1.4215	1.4227	1.4198	1.4211
	Ω_3	1.4871	1.4881	1.4857	1.4867	1.4844	1.4854
	Ω_4	1.6033	1.6040	1.6013	1.6020	1.5993	1.6000
	Ω_5	1.6874	1.6876	1.6857	1.6859	1.6840	1.6841
0.05 *L/a*=0.2	Ω_1	1.3151	1.3170	1.3125	1.3144	1.3099	1.3118
	Ω_2	1.4433	1.4451	1.4419	1.4437	1.4405	1.4422
	Ω_3	1.5404	1.5417	1.5387	1.5400	1.5370	1.5383
	Ω_4	1.6835	1.6835	1.6820	1.6820	16806	1.6805
	Ω_5	1.7259	1.7272	1.7237	1.7249	1.7214	1.7227
0.03 *L/a* =1	Ω_1	0.7805	0.7817	0.7785	0.7798	0.7765	0.7778
	Ω_2	0.8874	0.8890	0.8872	0.8887	0.8869	0.8885
	Ω_3	1.1753	1.1727	1.1737	1.1711	1.1721	1.1695
	Ω_4	1.3136	1.3145	1.3111	1.3120	1.3085	1.3094
	Ω_5	1.3325	1.3295	1.3314	1.3290	1.3301	1.3281
0.04 *L/a*=1	Ω_1	0.8694	0.8714	0.8672	0.8692	0.8650	0.8669
	Ω_2	1.0042	1.0066	1.0039	1.0063	1.0036	1.0060
	Ω_3	1.2880	1.2851	1.2861	1.2832	1.2842	1.2812
	Ω_4	1.3184	1.3201	1.3159	1.3175	1.3133	1.3150
	Ω_5	1.3528	1.3545	1.3505	1.3522	1.3482	1.3499
0.05 *L/a*=1	Ω_1	0.9489	0.9517	0.9465	0.9493	0.9441	0.9468
	Ω_2	1.1149	1.1181	1.1145	1.1178	1.1142	1.1174
	Ω_3	1.3231	1.3254	1.3206	1.3229	1.3181	1.3204
	Ω_4	1.3624	1.3638	1.3601	1.3616	1.3579	1.3593
	Ω_5	1.3807	1.3780	1.3785	1.3758	1.3763	1.3736

frequencies declined by increasing temperature. It seems that by increasing temperature, the variation of the non-zero harmonic natural frequencies is higher than the zeroth harmonic natural frequencies. Tables 5 and 6 show that the values of the ordinary terms of zeroth harmonic natural frequencies for both thin ring and thing hollow cylinder are higher than the values of complementary terms, first and second harmonic terms of natural frequencies; furthermore, the values of first and second harmonic natural frequencies are almost equal.

5. Conclusions

In this paper, the three-dimensional free vibration analysis of FGP circular structures under axial polarization and radial polarization are investigated by a semi-analytical mesh-free approach. In this approach, there is no need to make predefined meshes to model the structures; however, arbitrary distributed nodes are used to simulate the schemes. In addition, owing to use semi-analytical method, the

amount of computations are significantly reduced, and this method will be useful for 3D problems. In comparison with reference results in Table 1, validation study shows that the present results have approached to reference results quickly since few nodes are used for the whole structure for validation. There are two assumptions that help us to observe effect of temperature variations on the natural frequencies. First, by assuming that material properties depend on temperature, and second by considering nonlinear strain-displacement relationship. In this work, we assume that there is no dependency between temperature and properties to investigate separately effect of nonlinear relationship on the natural frequencies under temperature variations. If we did not consider nonlinear terms, temperature effect would appear as the external loads in equations, so temperature did not have any impact on the natural frequency then. Thus, by applying nonlinear terms, we showed that temperature can be explicitly appeared in stiffness matrices. After validation studies, the effects off different geometry parameters and temperature variations on non-dimensional natural frequencies are also studied. The non-dimensional natural frequencies decrease by temperature increasing regardless the type of structures, boundary conditions or type of polarization. Based on using the nonlinear Green-LaGrange relationship, the effects of temperature variations will be observed in stiffness matrices, and this consideration provides us the more accurate thermal analysis. As it is observed, the temperature variations do not have a noticeable effect on the natural frequencies. The non-dimensional natural frequencies of thin ring and hollow cylinder increase by increasing the ratio of thickness to outer radius. Also, natural frequencies of the structures decrease with increasing the ratio of the height of the structures to outer radius. The growth rate in complementary terms of zeroth harmonic natural frequencies (natural frequencies of pure warping modes) in radial polarization is higher than growth rate in the other terms of natural frequencies. In axial polarization, for low frequencies, the values of ordinary terms of natural frequencies (natural frequencies of symmetric modes) are higher than the values of the other terms of natural frequencies. In this article, the number of harmonics ($Nh = 0, 1\ and\ 2$) is limited to three, so Zeroth, first and second harmonic natural frequencies are not all of the natural frequencies. Thus, by increasing the number of harmonics, new natural frequencies can be obtained.

References

Allahverdizadeh, A., Naei, M. and Bahrami, M.N. (2008), "Vibration amplitude and thermal effects on the nonlinear behavior of thin circular functionally graded plates", *J. Mech. Sci.*, **50**(3), 445-454. https://doi.org/10.1016/j.ijmecsci.2007.09.018.

Almajid, A., Taya, M., Takagi, K., Li, J.-F. and Watanabe, R. (2002). "Fabrication and modeling of porous FGM piezoelectric actuators", *Smart Structures and Materials 2002: Smart Structures and Integrated Systems,* **5764**. https://doi.org/10.1117/12.474683

Amini, Y., Emdad, H. and Farid, M. (2015), "Finite element modeling of functionally graded piezoelectric harvesters", *Compos. Struct.*, **129**, 165-176. https://doi.org/10.1016/j.compstruct.2015.04.011.

Asgari, M. and Akhlaghi, M. (2010), "Transient thermal stresses in two-dimensional functionally graded thick hollow cylinder with finite length", *Arch. Appl. Mech.*, **80**(4), 353-376. https://doi.org/10.1007/s00419-009-0321-2.

Atluri, S.N., Kim, H.-G. and Cho, J.Y. (1999), "A critical assessment of the truly meshless local Petrov-Galerkin (MLPG), and local boundary integral equation (LBIE) methods", *Comput. Mech.*, **24**(5), 348-372. https://doi.org/10.1007/s004660050457.

Behjat, B. and Khoshravan, M. (2012), "Geometrically nonlinear static and free vibration analysis of functionally graded piezoelectric plates", *Compos. Struct.*, **94**(3), 874-882. https://doi.org/10.1016/j.compstruct.2011.08.024.

Behjat, B., Salehi, M., Sadighi, M., Armin, A. and Abbasi, M. (2009), "Static, dynamic, and free vibration analysis of functionally graded piezoelectric panels using finite element method", *J. Intelligent Mater. Syst. Struct.*, **20**(13), 1635-1646. https://doi.org/10.1177/1045389X09104113.

Benlahcen, F., Belakhdar, K., Sellami, M. and Tounsi, A. (2018), "Thermal buckling resistance of simply supported FGM plates with parabolic-concave thickness variation", *Steel Compos. Struct.*, **29**(5), 591-602. http://dx.doi.org/10.12989/scs.2017.25.2.187.

Bodaghi, M., Damanpack, A., Aghdam, M. and Shakeri, M. (2012), "Non-linear active control of FG beams in thermal environments subjected to blast loads with integrated FGP sensor/actuator layers", *Compos. Struct.*, **94**(12), 3612-3623. https://doi.org/10.1016/j.compstruct.2012.06.001.

Bodaghi, M. and Shakeri, M. (2012), "An analytical approach for free vibration and transient response of functionally graded piezoelectric cylindrical panels subjected to impulsive loads", *Compos. Struct.*, **94**(5), 1721-1735. https://doi.org/10.1016/j.compstruct.2012.01.009.

Chuaqui, T. and Roque, C. (2017), "Analysis of functionally graded piezoelectric Timoshenko smart beams using a multiquadric radial basis function method", *Compos. Struct.*, **176**, 640-653. https://doi.org/10.1016/j.compstruct.2017.05.062.

Dai, H.-L. and Rao, Y.-N. (2011), "Investigation on electromagnetothermoelastic interaction of functionally graded piezoelectric hollow spheres", *Struct. Eng. Mech.*, **40**(1), 49-64. http://dx.doi.org/10.12989/sem.2011.40.1.049.

Foroutan, M., Mohammadi, F., Alihemati, J. and Soltanimaleki, A. (2017), "Dynamic analysis of functionally graded piezoelectric cylindrical panels by a three-dimensional mesh-free model", *J. Intelligent Mater. Syst. Struct.*, **28**(18), 2516-2527. https://doi.org/10.1177/1045389X17689941.

Ghasemabadian, M. and Kadkhodayan, M. (2016), "Investigation of buckling behavior of functionally graded piezoelectric (FGP) rectangular plates under open and closed circuit conditions", *Struct. Eng. Mech.*, **60**(2), 271-299. http://dx.doi.org/10.12989/sem.2016.60.2.271.

Jodaei, A., Jalal, M. and Yas, M. (2013), "Three-dimensional free vibration analysis of functionally graded piezoelectric annular plates via SSDQM and comparative modeling by ANN", *Math. Comput. Model.*, **57**(5-6), 1408-1425. https://doi.org/10.1016/j.mcm.2012.12.002.

Khayat, M., Dehghan, S.M., Najafgholipour, M.A. and Baghlani, A. (2018), "Free vibration analysis of functionally graded cylindrical shells with different shell theories using semi-analytical method", *Steel Compos. Struct.*, **28**(6), 735-748. http://dx.doi.org/10.12989/scs.2018.28.6.735.

Koizumi, M. (1997), "FGM activities in Japan", *Compos. Part B Eng.*, **28**(1-2), 1-4. https://doi.org/10.1016/S1359-8368(96)00016-9.

Kruusing, A. (2000), "Analysis and optimization of loaded cantilever beam microactuators", *Smart Mater. Struct.*, **9**(2), 186. https://doi.org/10.1088/0964-1726/9/2/309

Lancaster, P. and Salkauskas, K. (1981), "Surfaces generated by

moving least squares methods", *Math. Comput.*, **37**(155), 141-158. https://doi.org/10.1090/S0025-5718-1981-0616367-1.

Larkin, K. and Abdelkefi, A. (2019), "Neutral axis modeling and effectiveness of functionally graded piezoelectric energy harvesters", *Compos. Struct.*, **213**, 25-36. https://doi.org/10.1016/j.compstruct.2019.01.067.

Lezgy-Nazargah, M., Vidal, P. and Polit, O. (2013), "An efficient finite element model for static and dynamic analyses of functionally graded piezoelectric beams", *Compos. Struct.*, **104**, 71-84. https://doi.org/10.1016/j.compstruct.2013.04.010.

Li, Y. and Shi, Z. (2009), "Free vibration of a functionally graded piezoelectric beam via state-space based differential quadrature", *Compos. Struct.*, **87**(3), 257-264. https://doi.org/10.1016/j.compstruct.2008.01.012.

Liu, C.-F. and Lee, Y.-T. (2000), "Finite element analysis of three-dimensional vibrations of thick circular and annular plates", *J. Sound Vib.*, **233**(1), 63-80. https://doi.org/10.1006/jsvi.1999.2791.

Liu, G.-R. and Gu, Y.-T. (2005), *An Introduction to Meshfree Methods and Their Programming*, Springer Science & Business Media, Germany.

Lü, C., Lim, C.W. and Chen, W. (2009), "Semi-analytical analysis for multi-directional functionally graded plates: 3-D elasticity solutions", *J. Numeric. Methods Eng.*, **79**(1), 25-44. https://doi.org/10.1002/nme.2555.

Mikaeeli, S. and Behjat, B. (2016), "Three-dimensional analysis of thick functionally graded piezoelectric plate using EFG method", *Compos. Struct.*, **154**, 591-599. https://doi.org/10.1016/j.compstruct.2016.07.067.

Nguyen, D.K. and Tran, T.T. (2018), "Free vibration of tapered BFGM beams using an efficient shear deformable finite element model", *Steel Compos. Struct.*, **29**(3), 363-377. http://dx.doi.org/10.12989/scs.2018.29.3.363.

Nie, G. and Zhong, Z. (2007), "Semi-analytical solution for three-dimensional vibration of functionally graded circular plates", *Comput. Methods Appl. Mech. Eng.*, **196**(49-52), 4901-4910. https://doi.org/10.1016/j.cma.2007.06.028.

Nie, G. and Zhong, Z. (2010), "Dynamic analysis of multi-directional functionally graded annular plates", *Appl. Math. Model.*, **34**(3), 608-616. https://doi.org/10.1016/j.apm.2009.06.009.

Priya, S. and Inman, D.J. (2009), *Energy Harvesting Technologies*, Springer, Germany. https://doi.org/10.1007/978-0- 387-76464-1.

Qian, L. and Batra, R. (2005), "Design of bidirectional functionally graded plate for optimal natural frequencies", *J. Sound Vib.*, **280**(1-2), 415-424. https://doi.org/10.1016/j.jsv.2004.01.042.

Qiu, J., Tani, J., Ueno, T., Morita, T., Takahashi, H. and Du, H. (2003), "Fabrication and high durability of functionally graded piezoelectric bending actuators", *Smart Mater. Struct.*, **12**(1), 115. https://doi.org/10.1088/0964-1726/12/1/313.

Sheng, G. and Wang, X. (2010), "Thermoelastic vibration and buckling analysis of functionally graded piezoelectric cylindrical shells", *Appl. Math. Model.*, **34**(9), 2630-2643. https://doi.org/10.1016/j.apm.2009.11.024.

Tsai, Y.-H. and Wu, C.-P. (2008), "Dynamic responses of functionally graded magneto-electro-elastic shells with open-circuit surface conditions", *J. Eng. Sci.*, **46**(9), 843-857. https://doi.org/10.1016/j.ijengsci.2008.03.005.

Wang, Y., Xu, R. and Ding, H. (2010), "Analytical solutions of functionally graded piezoelectric circular plates subjected to axisymmetric loads", *Acta Mechanica*, **215**(1-4), 287-305. https://doi.org/10.1007/s00707-010-0332-7.

Wu, C.-P. and Huang, H.-Y. (2019), "A semianalytical finite element method for stress and deformation analyses of bi-directional functionally graded truncated conical shells", *Mech. Based Design Struct. Machines*, 1-26. https://doi.org/10.1080/15397734.2019.1636657.

Wu, C.-P. and Li, H.-Y. (2013), "An RMVT-based finite rectangular prism method for the 3D analysis of sandwich FGM plates with various boundary conditions", *CMC-Comput. Mater. Continua*, **34**(1), 27-62. DOI:10.3970/cmc.2013.034.027.

Wu, C.-P. and Liu, Y.-C. (2016), "A review of semi-analytical numerical methods for laminated composite and multilayered functionally graded elastic/piezoelectric plates and shells", *Compos. Struct.*, **147**, 1-15. https://doi.org/10.1016/j.compstruct.2016.03.031.

Wu, C.-P. and Liu, Y.-C. (2016), "A state space meshless method for the 3D analysis of FGM axisymmetric circular plates", *Steel Compos. Struct.*, **22**(1), 161-182. https://doi.org/10.12989/scs.2016.22.1.161.

Wu, C.-P. and Tsai, Y.-H. (2009), "Cylindrical bending vibration of functionally graded piezoelectric shells using the method of perturbation", *J. Eng. Math.*, **63**(1), 95. https://doi.org/10.1007/s10665-008-9234-2.

Wu, C.-P. and Yang, S.-W. (2011), "A semi-analytical element-free Galerkin method for the 3D free vibration analysis of multilayered FGM circular hollow cylinders", *J. Intelligent Mater. Syst. Struct.*, **22**(17), 1993-2007. https://doi.org/10.1177/1045389X11421822.

Wu, C.C., Kahn, M. and Moy, W. (1996), "Piezoelectric ceramics with functional gradients: a new application in material design", *J. American Ceramic Soc.*, **79**(3), 809-812. https://doi.org/10.1111/j.11512916.1996.tb07951.x.

Wu, X.-H., Shen, Y.-P. and Chen, C. (2003), "An exact solution for functionally graded piezothermoelastic cylindrical shell as sensors or actuators", *Mater. Lett.*, **57**(22-23), 3532-3542. https://doi.org/10.1016/S0167-577X(03)00121-6.

Xiong, Q.-l. and Tian, X. (2017), "Transient thermo-piezo-elastic responses of a functionally graded piezoelectric plate under thermal shock", *Steel Compos. Struct.*, **25**(2), 187-196. http://dx.doi.org/10.12989/scs.2017.25.2.187.

Yas, M. and Moloudi, N. (2015), "Three-dimensional free vibration analysis of multi-directional functionally graded piezoelectric annular plates on elastic foundations via state space based differential quadrature method", *Appl. Math. Mech.*, **36**(4), 439-464. https://doi.org/10.1007/s10483-015-1923-9.

Zhong, Z. and Shang, E. (2003), "Three-dimensional exact analysis of a simply supported functionally gradient piezoelectric plate", *J. Solids Struct.*, **40**(20), 5335-5352. https://doi.org/10.1016/S0020-7683(03)00288-9.

Zhu, X. and Meng, Z. (1995), "Operational principle, fabrication and displacement characteristics of a functionally gradient piezoelectric ceramic actuator", *Sensors Actuators A Phys.*, **48**(3), 169-176. https://doi.org/10.1016/0924-4247(95)00996-5.

CC

Appendix A

$$\widehat{KE}_{1n}^{UU} = \int (\bar{\theta}_n N_U)^T \rho \bar{\theta}_n N_U d\Omega_i \ , \widehat{KE}_{2n}^{UU} = \int (\bar{\theta}_n N_U)^T \rho \bar{\bar{\theta}}_n N_U d\Omega_i$$

$$\widehat{KE}_{3n}^{UU} = \int \left(\bar{\bar{\theta}}_n N_U\right)^T \rho \bar{\theta}_n N_U d\Omega_i \ , \widehat{KE}_{4n}^{UU} = \int \left(\bar{\bar{\theta}}_n N_U\right)^T \rho \bar{\bar{\theta}}_n N_U d\Omega_i$$

Appendix B

$$\sum_{i=1}^{NG} \int (\delta S^T C^E S) d\Omega_i = \sum_{i=1}^{NG} \int \left[\left(\sum_{n=0}^{NG} \delta \left(L_U \bar{\theta}_n N_U \hat{\bar{q}}_n + L_U \bar{\bar{\theta}}_n N_U \hat{\bar{\bar{q}}}_n \right)^T \right) C^E \left(\sum_{n=0}^{NG} \left(L_U \bar{\theta}_n N_U \hat{\bar{q}}_n + L_U \bar{\bar{\theta}}_n N_U \hat{\bar{\bar{q}}}_n \right) \right) \right] d\Omega_i$$

$$\sum_{i=1}^{NG} \int (\delta S^T e^T E) d\Omega_i = \sum_{i=1}^{Ne} \int \left[\left(\sum_{n=0}^{NG} \delta \left(L_U \bar{\theta}_n N_U \hat{\bar{q}}_n + L_U \bar{\bar{\theta}}_n N_U \hat{\bar{\bar{q}}}_n \right)^T \right) e^T \left(\sum_{n=0}^{NG} \left(-L_\Phi cosn\theta N_\Phi \hat{\bar{\phi}}_n - L_\Phi sinn\theta N_\Phi \hat{\bar{\bar{\phi}}}_n \right) \right) \right] d\Omega_i$$

$$\sum_{i=1}^{NG} \int (\delta S^T C^E \alpha \Delta T) d\Omega_i = \sum_{i=1}^{NG} \int \left[\left((\delta N L_U)^T + \sum_{n=0}^{Nh} \delta \left(L_U \bar{\theta}_n N_U \hat{\bar{q}}_n + L_U \bar{\bar{\theta}}_n N_U \hat{\bar{\bar{q}}}_n \right)^T \right) C^E \alpha \Delta T \right] d\Omega_i$$

$$\sum_{i=1}^{NG} \int (\delta E^T e S) d\Omega_i = \sum_{i=1}^{NG} \int \left[\left(\sum_{n=0}^{Nh} \delta \left(-L_\Phi cosn\theta N_\Phi \hat{\bar{\phi}}_n - L_\Phi sinn\theta N_\Phi \hat{\bar{\bar{\phi}}}_n \right)^T \right) e \left(\sum_{n=0}^{Nh} \left(L_u \bar{\theta}_n N_U \hat{\bar{q}}_n + L_u \bar{\bar{\theta}}_n N_U \hat{\bar{\bar{q}}}_n \right) \right) \right] d\Omega_i$$

$$\sum_{i=1}^{NG} \int (\delta E^T \xi E) d\Omega_i = \sum_{i=1}^{NG} \int \left[\left(\sum_{n=0}^{Nh} \delta \left(-L_\Phi cosn\theta N_\Phi \hat{\bar{\phi}}_n - L_\Phi sinn\theta N_\Phi \hat{\bar{\bar{\phi}}}_n \right)^T \right) \xi \left(\sum_{n=0}^{Nh} \left(-L_\Phi cosn\theta N_\Phi \hat{\bar{\phi}}_n - L_\Phi sinn\theta N_\Phi \hat{\bar{\bar{\phi}}}_n \right) \right) \right] d\Omega_i$$

$$\sum_{i=1}^{NG} \int (\delta E^T p \Delta T) d\Omega_i = -\sum_{i=1}^{NG} \sum_{n=0}^{Nh} \int \left[\left(\delta \hat{\bar{\phi}}_n \right)^T {N_\Phi}^T cosn\theta {L_\Phi}^T p \Delta T + \left(\delta \hat{\bar{\bar{\phi}}}_n \right)^T {N_\Phi}^T sinn\theta {L_\Phi}^T p \Delta T \right] d\Omega_i$$

Appendix C

$$\delta W = \int \left(\delta U^T \hat{F}_{\boldsymbol{b}} + \delta \Phi^T \hat{Q}_b \right) d\Omega + \int (\delta U^T \hat{F}_{\boldsymbol{s}} + \delta \Phi^T \hat{Q}_s) dS$$

$$= \sum_{i=1}^{NG} \left[\int \left(\sum_{n=0}^{Nh} \delta \left(\bar{\theta}_n N_U \hat{\bar{q}}_n + \bar{\bar{\theta}}_n N_U \hat{\bar{\bar{q}}}_n \right)^T \right) \left(\sum_{n=0}^{Nh} \left(\bar{\theta}_n \hat{\bar{F}}_{bn} + \bar{\bar{\theta}}_n \hat{\bar{\bar{F}}}_{bn} \right) \right) d\Omega_i \right.$$

$$+ \int \left(\sum_{n=0}^{Nh} \delta \left(\bar{\theta}_n N_U \hat{\bar{q}}_n + \bar{\bar{\theta}}_n N_U \hat{\bar{\bar{q}}}_n \right)^T \right) \left(\sum_{n=0}^{Nh} \left(\bar{\theta}_n \hat{\bar{F}}_{sn} + \bar{\bar{\theta}}_n \hat{\bar{\bar{F}}}_{sn} \right) \right) ds_i$$

$$+ \int \left(\sum_{n=0}^{Nh} \delta \left(cosn\theta N_\Phi \hat{\bar{\phi}}_n + sinn\theta N_\Phi \hat{\bar{\bar{\phi}}}_n \right)^T \right) \left(\sum_{n=0}^{Nh} \left(cosn\theta \hat{\bar{Q}}_{bn} + sinn\theta \hat{\bar{\bar{Q}}}_{bn} \right) \right) d\Omega_i$$

$$\left. + \int \left(\sum_{n=0}^{Nh} \delta \begin{pmatrix} cosn\theta N_\Phi \hat{\bar{\phi}}_n \\ +sinn\theta N_\Phi \hat{\bar{\bar{\phi}}}_n \end{pmatrix}^T \right) \left(\sum_{n=0}^{Nh} \left(cosn\theta \hat{\bar{Q}}_{sn} + sinn\theta \hat{\bar{\bar{Q}}}_{sn} \right) \right) ds_i \right] \rightarrow$$

and

$$\sum_{i=1}^{NG} \sum_{n=0}^{Nh} \left[\delta \hat{\bar{q}}_n^T \hat{F}_1^b + \delta \hat{\bar{\bar{q}}}_n^T \hat{F}_2^b + \delta \hat{\bar{q}}_n^T \hat{F}_1^s + \delta \hat{\bar{\bar{q}}}_n^T \hat{F}_2^s + \delta \hat{\bar{\phi}}_n^T \hat{Q}_1^b + \delta \hat{\bar{\bar{\phi}}}_n^T \hat{Q}_2^b + \delta \hat{\bar{\phi}}_n^T \hat{Q}_1^s + \delta \hat{\bar{\bar{\phi}}}_n^T \hat{Q}_2^s \right]$$

$\hat{F}_1^b$, $\hat{F}_1^s$, $\hat{Q}_1^b$ and $\hat{Q}_1^s$ are the mechanical body force, mechanical surface force, electrical body force and electrical surface force which can be described as below:

$$\hat{F}_1^b = \int (\bar{\theta}_n N_U)^T \left(\bar{\theta}_n \hat{\bar{F}}_{bn} + \bar{\bar{\theta}}_n \hat{\bar{\bar{F}}}_{bn}\right) d\Omega_i \ , \hat{F}_2^b = \int \left(\bar{\bar{\theta}}_n N_U\right)^T \left(\bar{\theta}_n \hat{\bar{F}}_{bn} + \bar{\bar{\theta}}_n \hat{\bar{\bar{F}}}_{bn}\right) d\Omega_i$$

$$\hat{F}_1^s = \int (\bar{\theta}_n N_U)^T \left(\bar{\theta}_n \hat{\bar{F}}_{sn} + \bar{\bar{\theta}}_n \hat{\bar{\bar{F}}}_{sn}\right) ds_i \ , \hat{F}_2^s = \int \left(\bar{\bar{\theta}}_n N_U\right)^T \left(\bar{\theta}_n \hat{\bar{F}}_{sn} + \bar{\bar{\theta}}_n \hat{\bar{\bar{F}}}_{sn}\right) ds_i$$

$$\hat{Q}_1^b = \int (cosn\theta N_\Phi)^T \left(cosn\theta \hat{Q}_{bn} + sinn\theta \hat{\bar{Q}}_{bn}\right) d\Omega_i \ ,$$

$$\hat{Q}_2^b = \int (sinn\theta N_\Phi)^T \left(cosn\theta \hat{Q}_{bn} + sinn\theta \hat{\bar{Q}}_{bn}\right) d\Omega_i$$

$$\hat{Q}_1^s = \int (cosn\theta N_\Phi)^T \left(cosn\theta \hat{Q}_{sn} + sinn\theta \hat{\bar{Q}}_{sn}\right) ds_i$$

$$\hat{Q}_2^s = \int (sinn\theta N_\Phi)^T (cosn\theta \hat{Q}_{sn} + sinn\theta \hat{\bar{Q}}_{sn}) ds_i$$

Appendix D

$$\begin{aligned}\delta H = \sum_{i=1}^{NG}\sum_{n=0}^{Nh}\Big[&\left(\delta\hat{q}_n\right)^T \hat{H}_{1n}^{UU}\hat{q}_n + \left(\delta\hat{q}_n\right)^T \hat{H}_{2n}^{UU}\hat{\bar{q}}_n \\ &+ \left(\delta\hat{\bar{q}}_n\right)^T \hat{H}_{3n}^{UU}\hat{q}_n + \left(\delta\hat{\bar{q}}_n\right)^T \hat{H}_{4n}^{UU}\hat{\bar{q}}_n \\ &+ \left(\delta\hat{q}_n\right)^T \hat{H}_{1n}^{U\Phi}\hat{\phi}_n + \left(\delta\hat{q}_n\right)^T \hat{H}_{2n}^{U\Phi}\hat{\bar{\phi}}_n \\ &+ \left(\delta\hat{\bar{q}}_n\right)^T \hat{H}_{3n}^{U\Phi}\hat{\phi}_n + \left(\delta\hat{\bar{q}}_n\right)^T \hat{H}_{4n}^{U\Phi}\hat{\bar{\phi}}_n \\ &- \left(\delta\hat{q}_n\right)^T \hat{H}_{1n}^{U\Delta T}\hat{q}_n - \left(\delta\hat{q}_n\right)^T \hat{H}_{2n}^{U\Delta T}\hat{\bar{q}}_n \\ &- \left(\delta\hat{\bar{q}}_n\right)^T \hat{H}_{3n}^{U\Delta T}\hat{q}_n - \left(\delta\hat{\bar{q}}_n\right)^T \hat{H}_{4n}^{U\Delta T}\hat{\bar{q}}_n \\ &- \left(\delta\hat{q}_n\right)^T \hat{F}_{1n}^{\Delta T} - \left(\delta\hat{\bar{q}}_n\right)^T \hat{F}_{2n}^{\Delta T} \\ &+ \left(\delta\hat{\phi}_n\right)^T \hat{H}_{1n}^{\Phi U}\hat{q}_n + \left(\delta\hat{\phi}_n\right)^T \hat{H}_{2n}^{\Phi U}\hat{\bar{q}}_n \\ &+ \left(\delta\hat{\bar{\phi}}_n\right)^T \hat{H}_{3n}^{\Phi U}\hat{q}_n + \left(\delta\hat{\bar{\phi}}_n\right)^T \hat{H}_{4n}^{\Phi U}\hat{\bar{q}}_n \\ &- \left(\delta\hat{\phi}_n\right)^T \hat{H}_{1n}^{\Phi\Phi}\hat{\phi}_n - \left(\delta\hat{\phi}_n\right)^T \hat{H}_{2n}^{\Phi\Phi}\hat{\bar{\phi}}_n \\ &- \left(\delta\hat{\bar{\phi}}_n\right)^T \hat{H}_{3n}^{\Phi\Phi}\hat{\phi}_n - \left(\delta\hat{\bar{\phi}}_n\right)^T \hat{H}_{4n}^{\Phi\Phi}\hat{\bar{\phi}}_n \\ &+ \left(\delta\hat{\phi}_n\right)^T \hat{Q}_{1n}^{\Delta T} + \left(\delta\hat{\bar{\phi}}_n\right)^T \hat{Q}_{2n}^{\Delta T}\Big]\end{aligned}$$

$$\hat{H}_{1n}^{UU} = \int (L_U\bar{\theta}_n N_U)^T C^E L_U \bar{\theta}_n N_U d\Omega_i \ , \hat{H}_{2n}^{UU} = \int (L_U\bar{\theta}_n N_U)^T C^E L_U \bar{\bar{\theta}}_n N_U d\Omega_i$$

$$\hat{H}_{3n}^{UU} = \int \left(L_U\bar{\bar{\theta}}_n N_U\right)^T C^E L_U \bar{\theta}_n N_U d\Omega_i \ , \hat{H}_{4n}^{UU} = \int \left(L_U\bar{\bar{\theta}}_n N_U\right)^T C^E L_U \bar{\bar{\theta}}_n N_U d\Omega_i$$

$$\hat{H}_{1n}^{U\psi} = \int (L_U\bar{\theta}_n N_U)^T e^T L_\Phi cos\frac{n\pi}{\Theta}\theta N_\Phi d\Omega_i \ , \hat{H}_{2n}^{U\psi} = \int (L_U\bar{\theta}_n N_U)^T e^T L_\Phi sin\frac{n\pi}{\Theta}\theta N_\Phi d\Omega_i$$

$$\hat{H}_{3n}^{U\psi} = \int \left(L_U\bar{\bar{\theta}}_n N_U\right)^T e^T L_\Phi cos\frac{n\pi}{\Theta}\theta N_\Phi d\Omega_i \ , \hat{H}_{4n}^{U\psi} = \int \left(L_U\bar{\bar{\theta}}_n N_U\right)^T e^T L_\Phi sin\frac{n\pi}{\Theta}\theta N_\Phi d\Omega_i$$

$$\hat{H}_{1n}^{\psi U} = \int \left(L_\Phi cos\frac{n\pi}{\Theta}\theta N_\Phi\right)^T eL_U\bar{\theta}_n N_U d\Omega_i \ , \hat{H}_{2n}^{\psi U} = \int \left(L_\Phi cos\frac{n\pi}{\Theta}\theta N_\Phi\right)^T eL_U\bar{\bar{\theta}}_n N_U d\Omega_i$$

$$\hat{H}_{3n}^{\psi U} = \int \left(L_\Phi sin\frac{n\pi}{\Theta}\theta N_\Phi\right)^T eL_U\bar{\theta}_n N_U d\Omega_i \ , \hat{H}_{4n}^{\psi U} = \int \left(L_\Phi sin\frac{n\pi}{\Theta}\theta N_\Phi\right)^T eL_U\bar{\bar{\theta}}_n N_U d\Omega_i$$

$$\hat{H}_{1n}^{\psi\psi} = \int \left(L_\Phi cos\frac{n\pi}{\Theta}\theta N_\Phi\right)^T \xi L_\phi cos\frac{n\pi}{\Theta}\theta N_\Phi d\Omega_i \ , \hat{H}_{2n}^{\psi\psi} = \int \left(L_\Phi cos\frac{n\pi}{\Theta}\theta N_\Phi\right)^T \xi L_\Phi sin\frac{n\pi}{\Theta}\theta N_\Phi d\Omega_i$$

$$\hat{H}_{3n}^{\psi\psi} = \int \left(L_\Phi sin\frac{n\pi}{\Theta}\theta N_\Phi\right)^T \xi L_\phi cos\frac{n\pi}{\Theta}\theta N_\Phi d\Omega_i \ , \hat{H}_{4n}^{\psi\psi} = \int \left(L_\Phi sin\frac{n\pi}{\Theta}\theta N_\Phi\right)^T \xi L_\Phi sin\frac{n\pi}{\Theta}\theta N_\Phi d\Omega_i$$

$$\hat{F}_{1n}^{\Delta T} = \int (L_U\bar{\theta}_n N_U)^T \beta\Delta T d\Omega_i \ , \hat{F}_{2n}^{\Delta T} = \int \left(L_U\bar{\bar{\theta}}_n N_U\right)^T \beta\Delta T d\Omega_i$$

$$\hat{Q}_{1n}^{\Delta T} = \int \left(L_\Phi cos\frac{n\pi}{\Theta}\theta N_\Phi\right)^T p\Delta T d\Omega_i \ , \hat{Q}_{2n}^{\Delta T} = \int \left(L_\Phi sin\frac{n\pi}{\Theta}\theta N_\Phi\right)^T p\Delta T d\Omega_i$$

$$\hat{H}_{1n}^{U\Delta T} = \int \Delta T \begin{bmatrix} A_{11} & \dots & A_{1N_n} \\ \vdots & \ddots & \vdots \\ A_{N_n1} & \cdots & A_{N_nN_n}\end{bmatrix} d\Omega_i \ , \hat{H}_{2n}^{U\Delta T} = \int \Delta T \begin{bmatrix} B_{11} & \dots & B_{1N_n} \\ \vdots & \ddots & \vdots \\ B_{N_n1} & \cdots & B_{N_nN_n}\end{bmatrix} d\Omega_i$$

$$\hat{H}_{3n}^{U\Delta T} = \int \Delta T \begin{bmatrix} C_{11} & \dots & C_{1N_n} \\ \vdots & \ddots & \vdots \\ C_{N_n1} & \cdots & C_{N_nN_n}\end{bmatrix} d\Omega_i \ , \hat{H}_{4n}^{U\Delta T} = \int \Delta T \begin{bmatrix} D_{11} & \dots & D_{1N_n} \\ \vdots & \ddots & \vdots \\ D_{N_n1} & \cdots & D_{N_nN_n}\end{bmatrix} d\Omega_i$$

Where

$$A_{ij} = \begin{bmatrix} A_{ij}(1,1) & A_{ij}(1,2) & 0 \\ A_{ij}(2,1) & A_{ij}(2,2) & 0 \\ 0 & 0 & A_{ij}(3,3)\end{bmatrix}$$

$$B_{ij}=\begin{bmatrix} B_{ij}(1,1) & B_{ij}(1,2) & 0 \\ B_{ij}(2,1) & B_{ij}(2,2) & 0 \\ 0 & 0 & B_{ij}(3,3) \end{bmatrix}$$

$$C_{ij}=\begin{bmatrix} C_{ij}(1,1) & C_{ij}(1,2) & 0 \\ C_{ij}(2,1) & C_{ij}(2,2) & 0 \\ 0 & 0 & C_{ij}(3,3) \end{bmatrix}$$

$$D_{ij}=\begin{bmatrix} D_{ij}(1,1) & D_{ij}(1,2) & 0 \\ D_{ij}(2,1) & D_{ij}(2,2) & 0 \\ 0 & 0 & D_{ij}(3,3) \end{bmatrix}$$

and

$$\begin{aligned} A_{ij}(1,1) = {} & \tfrac{\partial N_i^U}{\partial r}\bar{\theta}_n(1,1)\beta_1\tfrac{\partial N_j^U}{\partial r}\bar{\theta}_n(1,1) \\ & + \frac{N_i^U}{r}\bar{\theta}_n(1,1)\beta_2\frac{N_j^U}{r}\bar{\theta}_n(1,1) + \frac{N_i^U}{r}\frac{\partial\bar{\theta}_n(1,1)}{\partial\theta}\beta_2\frac{N_j^U}{r}\frac{\partial\bar{\theta}_n(1,1)}{\partial\theta} \\ & + \frac{\partial N_i^U}{\partial z}\bar{\theta}_n(1,1)\beta_3\frac{\partial N_j^U}{\partial z}\bar{\theta}_n(1,1) \\ & + \frac{N_i^U}{r}\frac{\partial\bar{\theta}_n(1,1)}{\partial\theta}\beta_4\frac{\partial N_j^U}{\partial r}\bar{\theta}_n(1,1) \\ & + \frac{\partial N_i^U}{\partial r}\bar{\theta}_n(1,1)\beta_4\frac{N_j^U}{r}\frac{\partial\bar{\theta}_n(1,1)}{\partial\theta} \\ & + \frac{N_i^U}{r}\frac{\partial\bar{\theta}_n(1,1)}{\partial\theta}\beta_5\frac{\partial N_j^U}{\partial z}\bar{\theta}_n(1,1) \\ & + \frac{\partial N_i^U}{\partial z}\bar{\theta}_n(1,1)\beta_5\frac{N_j^U}{r}\frac{\partial\bar{\theta}_n(1,1)}{\partial\theta} \\ & + \frac{\partial N_i^U}{\partial r}\bar{\theta}_n(1,1)\beta_6\frac{\partial N_j^U}{\partial z}\bar{\theta}_n(1,1) \\ & + \frac{\partial N_i^U}{\partial z}\bar{\theta}_n(1,1)\beta_6\frac{\partial N_j^U}{\partial r}\bar{\theta}_n(1,1) \end{aligned}$$

$$\begin{aligned} A_{ij}(1,2) = {} & \tfrac{N_i^U}{r}\bar{\theta}_n(1,1)\beta_2\tfrac{N_j^U}{r}\tfrac{\partial\bar{\theta}_n(2,2)}{\partial\theta} \\ & - \frac{N_i^U}{r}\frac{\partial\bar{\theta}_n(1,1)}{\partial\theta}\beta_2\frac{N_j^U}{r}\bar{\theta}_n(2,2) \\ & + \frac{N_i^U}{r}\bar{\theta}_n(1,1)\beta_4\frac{\partial N_j^U}{\partial r}\bar{\theta}_n(2,2) \\ & - \frac{\partial N_i^U}{\partial r}\bar{\theta}_n(1,1)\beta_4\frac{N_j^U}{r}\bar{\theta}_n(2,2) \\ & + \frac{N_i^U}{r}\bar{\theta}_n(1,1)\beta_5\frac{\partial N_j^U}{\partial z}\bar{\theta}_n(2,2) \\ & - \frac{\partial N_i^U}{\partial z}\bar{\theta}_n(1,1)\beta_5\frac{N_j^U}{r}\bar{\theta}_n(2,2) \end{aligned}$$

$$\begin{aligned} A_{ij}(2,1) = {} & -\tfrac{N_i^U}{r}\bar{\theta}_n(2,2)\beta_2\tfrac{N_j^U}{r}\tfrac{\partial\bar{\theta}_n(1,1)}{\partial\theta} \\ & + \frac{N_i^U}{r}\frac{\partial\bar{\theta}_n(2,2)}{\partial\theta}\beta_2\frac{N_j^U}{r}\bar{\theta}_n(1,1) \\ & - \frac{N_i^U}{r}\bar{\theta}_n(2,2)\beta_4\frac{\partial N_j^U}{\partial r}\bar{\theta}_n(1,1) \\ & + \frac{\partial N_i^U}{\partial r}\bar{\theta}_n(2,2)\beta_4\frac{N_j^U}{r}\bar{\theta}_n(1,1) \\ & - \frac{N_i^U}{r}\bar{\theta}_n(2,2)\beta_5\frac{\partial N_j^U}{\partial z}\bar{\theta}_n(1,1) \\ & + \frac{\partial N_i^U}{\partial z}\bar{\theta}_n(2,2)\beta_5\frac{N_j^U}{r}\bar{\theta}_n(1,1) \end{aligned}$$

$$\begin{aligned} A_{ij}(2,2) = {} & \frac{\partial N_i^U}{\partial r}\bar{\theta}_n(2,2)\beta_1\frac{\partial N_j^U}{\partial r}\bar{\theta}_n(2,2) \\ & + \frac{N_i^U}{r}\bar{\theta}_n(2,2)\beta_2\frac{N_j^U}{r}\bar{\theta}_n(2,2) \\ & + \frac{N_i^U}{r}\frac{\partial\bar{\theta}_n(2,2)}{\partial\theta}\beta_2\frac{N_j^U}{r}\frac{\partial\bar{\theta}_n(2,2)}{\partial\theta} \\ & + \frac{\partial N_i^U}{\partial z}\bar{\theta}_n(2,2)\beta_3\frac{\partial N_j^U}{\partial z}\bar{\theta}_n(2,2) \\ & + \frac{N_i^U}{r}\frac{\partial\bar{\theta}_n(2,2)}{\partial\theta}\beta_4\frac{\partial N_j^U}{\partial r}\bar{\theta}_n(2,2) \\ & + \frac{\partial N_i^U}{\partial r}\bar{\theta}_n(2,2)\beta_4\frac{N_j^U}{r}\frac{\partial\bar{\theta}_n(2,2)}{\partial\theta} \\ & + \frac{N_i^U}{r}\frac{\partial\bar{\theta}_n(2,2)}{\partial\theta}\beta_5\frac{\partial N_j^U}{\partial z}\bar{\theta}_n(2,2) \\ & + \frac{\partial N_i^U}{\partial z}\bar{\theta}_n(2,2)\beta_5\frac{N_j^U}{r}\frac{\partial\bar{\theta}_n(2,2)}{\partial\theta} \\ & + \frac{\partial N_i^U}{\partial r}\bar{\theta}_n(2,2)\beta_6\frac{\partial N_j^U}{\partial z}\bar{\theta}_n(2,2) \\ & + \frac{\partial N_i^U}{\partial z}\bar{\theta}_n(2,2)\beta_6\frac{\partial N_j^U}{\partial r}\bar{\theta}_n(2,2) \end{aligned}$$

$$\begin{aligned} A_{ij}(3,3) = {} & \frac{\partial N_i^U}{\partial r}\bar{\theta}_n(3,3)\beta_1\frac{\partial N_j^U}{\partial r}\bar{\theta}_n(3,3) \\ & + \frac{N_i^U}{r}\frac{\partial\bar{\theta}_n(3,3)}{\partial\theta}\beta_2\frac{N_j^U}{r}\frac{\partial\bar{\theta}_n(3,3)}{\partial\theta} \\ & + \frac{\partial N_i^U}{\partial z}\bar{\theta}_n(3,3)\beta_3\frac{\partial N_j^U}{\partial z}\bar{\theta}_n(3,3) \\ & + \frac{N_i^U}{r}\frac{\partial\bar{\theta}_n(3,3)}{\partial\theta}\beta_4\frac{\partial N_j^U}{\partial r}\bar{\theta}_n(3,3) \\ & + \frac{\partial N_i^U}{\partial r}\bar{\theta}_n(3,3)\beta_4\frac{N_j^U}{r}\frac{\partial\bar{\theta}_n(3,3)}{\partial\theta} \\ & + \frac{N_i^U}{r}\frac{\partial\bar{\theta}_n(3,3)}{\partial\theta}\beta_5\frac{\partial N_j^U}{\partial z}\bar{\theta}_n(3,3) \\ & + \frac{\partial N_i^U}{\partial z}\bar{\theta}_n(3,3)\beta_5\frac{N_j^U}{r}\frac{\partial\bar{\theta}_n(3,3)}{\partial\theta} \\ & + \frac{\partial N_i^U}{\partial r}\bar{\theta}_n(3,3)\beta_6\frac{\partial N_j^U}{\partial z}\bar{\theta}_n(3,3) \\ & + \frac{\partial N_i^U}{\partial z}\bar{\theta}_n(3,3)\beta_6\frac{\partial N_j^U}{\partial r}\bar{\theta}_n(3,3) \end{aligned}$$

$$\begin{aligned} B_{ij}(1,1) = {} & \frac{\partial N_i^U}{\partial r}\bar{\theta}_n(1,1)\beta_1\frac{\partial N_j^U}{\partial r}\bar{\bar{\theta}}_n(1,1) \\ & + \frac{N_i^U}{r}\bar{\theta}_n(1,1)\beta_2\frac{N_j^U}{r}\bar{\bar{\theta}}_n(1,1) \\ & + \frac{N_i^U}{r}\frac{\partial\bar{\theta}_n(1,1)}{\partial\theta}\beta_2\frac{N_j^U}{r}\frac{\partial\bar{\bar{\theta}}_n(1,1)}{\partial\theta} \\ & + \frac{\partial N_i^U}{\partial z}\bar{\theta}_n(1,1)\beta_3\frac{\partial N_j^U}{\partial z}\bar{\bar{\theta}}_n(1,1) \\ & + \frac{N_i^U}{r}\frac{\partial\bar{\theta}_n(1,1)}{\partial\theta}\beta_4\frac{\partial N_j^U}{\partial r}\bar{\bar{\theta}}_n(1,1) \\ & + \frac{\partial N_i^U}{\partial r}\bar{\theta}_n(1,1)\beta_4\frac{N_j^U}{r}\frac{\partial\bar{\bar{\theta}}_n(1,1)}{\partial\theta} \\ & + \frac{N_i^U}{r}\frac{\partial\bar{\theta}_n(1,1)}{\partial\theta}\beta_5\frac{\partial N_j^U}{\partial z}\bar{\bar{\theta}}_n(1,1) \\ & + \frac{\partial N_i^U}{\partial z}\bar{\theta}_n(1,1)\beta_5\frac{N_j^U}{r}\frac{\partial\bar{\bar{\theta}}_n(1,1)}{\partial\theta} \\ & + \frac{\partial N_i^U}{\partial r}\bar{\theta}_n(1,1)\beta_6\frac{\partial N_j^U}{\partial z}\bar{\bar{\theta}}_n(1,1) \\ & + \frac{\partial N_i^U}{\partial z}\bar{\theta}_n(1,1)\beta_6\frac{\partial N_j^U}{\partial r}\bar{\bar{\theta}}_n(1,1) \end{aligned}$$

$$B_{ij}(1,2) = \frac{N_i^U}{r}\bar{\theta}_n(1,1)\beta_2\frac{N_j^U}{r}\frac{\partial\bar{\bar{\theta}}_n(2,2)}{\partial\theta} - \frac{N_i^U}{r}\frac{\partial\bar{\theta}_n(1,1)}{\partial\theta}\beta_2\frac{N_j^U}{r}\bar{\bar{\theta}}_n(2,2) + \frac{N_i^U}{r}\bar{\theta}_n(1,1)\beta_4\frac{\partial N_j^U}{\partial r}\bar{\bar{\theta}}_n(2,2) - \frac{\partial N_i^U}{\partial r}\bar{\theta}_n(1,1)\beta_4\frac{N_j^U}{r}\bar{\bar{\theta}}_n(2,2) + \frac{N_i^U}{r}\bar{\theta}_n(1,1)\beta_5\frac{\partial N_j^U}{\partial z}\bar{\bar{\theta}}_n(2,2) - \frac{\partial N_i^U}{\partial z}\bar{\theta}_n(1,1)\beta_5\frac{N_j^U}{r}\bar{\bar{\theta}}_n(2,2)$$

$$B_{ij}(2,1) = -\frac{N_i^U}{r}\bar{\theta}_n(2,2)\beta_2\frac{N_j^U}{r}\frac{\partial\bar{\bar{\theta}}_n(1,1)}{\partial\theta} + \frac{N_i^U}{r}\frac{\partial\bar{\theta}_n(2,2)}{\partial\theta}\beta_2\frac{N_j^U}{r}\bar{\bar{\theta}}_n(1,1) - \frac{N_i^U}{r}\bar{\theta}_n(2,2)\beta_4\frac{\partial N_j^U}{\partial r}\bar{\bar{\theta}}_n(1,1) + \frac{\partial N_i^U}{\partial r}\bar{\theta}_n(2,2)\beta_4\frac{N_j^U}{r}\bar{\bar{\theta}}_n(1,1) - \frac{N_i^U}{r}\bar{\theta}_n(2,2)\beta_5\frac{\partial N_j^U}{\partial z}\bar{\bar{\theta}}_n(1,1) + \frac{\partial N_i^U}{\partial z}\bar{\theta}_n(2,2)\beta_5\frac{N_j^U}{r}\bar{\bar{\theta}}_n(1,1)$$

$$B_{ij}(2,2) = \frac{\partial N_i^U}{\partial r}\bar{\theta}_n(2,2)\beta_1\frac{\partial N_j^U}{\partial r}\bar{\bar{\theta}}_n(2,2) + \frac{N_i^U}{r}\bar{\theta}_n(2,2)\beta_2\frac{N_j^U}{r}\bar{\bar{\theta}}_n(2,2) + \frac{N_i^U}{r}\frac{\partial\bar{\theta}_n(2,2)}{\partial\theta}\beta_2\frac{N_j^U}{r}\frac{\partial\bar{\bar{\theta}}_n(2,2)}{\partial\theta} + \frac{\partial N_i^U}{\partial z}\bar{\theta}_n(2,2)\beta_3\frac{\partial N_j^U}{\partial z}\bar{\bar{\theta}}_n(2,2) + \frac{N_i^U}{r}\frac{\partial\bar{\theta}_n(2,2)}{\partial\theta}\beta_4\frac{\partial N_j^U}{\partial r}\bar{\bar{\theta}}_n(2,2) + \frac{\partial N_i^U}{\partial r}\bar{\theta}_n(2,2)\beta_4\frac{N_j^U}{r}\frac{\partial\bar{\bar{\theta}}_n(2,2)}{\partial\theta} + \frac{N_i^U}{r}\frac{\partial\bar{\theta}_n(2,2)}{\partial\theta}\beta_5\frac{\partial N_j^U}{\partial z}\bar{\bar{\theta}}_n(2,2) + \frac{\partial N_i^U}{\partial z}\bar{\theta}_n(2,2)\beta_5\frac{N_j^U}{r}\frac{\partial\bar{\bar{\theta}}_n(2,2)}{\partial\theta} + \frac{\partial N_i^U}{\partial r}\bar{\theta}_n(2,2)\beta_6\frac{\partial N_j^U}{\partial z}\bar{\bar{\theta}}_n(2,2) + \frac{\partial N_i^U}{\partial z}\bar{\theta}_n(2,2)\beta_6\frac{\partial N_j^U}{\partial r}\bar{\bar{\theta}}_n(2,2)$$

$$B_{ij}(3,3) = \frac{\partial N_i^U}{\partial r}\bar{\theta}_n(3,3)\beta_1\frac{\partial N_j^U}{\partial r}\bar{\bar{\theta}}_n(3,3) + \frac{N_i^U}{r}\frac{\partial\bar{\theta}_n(3,3)}{\partial\theta}\beta_2\frac{N_j^U}{r}\frac{\partial\bar{\bar{\theta}}_n(3,3)}{\partial\theta} + \frac{\partial N_i^U}{\partial z}\bar{\theta}_n(3,3)\beta_3\frac{\partial N_j^U}{\partial z}\bar{\bar{\theta}}_n(3,3) + \frac{N_i^U}{r}\frac{\partial\bar{\theta}_n(3,3)}{\partial\theta}\beta_4\frac{\partial N_j^U}{\partial r}\bar{\bar{\theta}}_n(3,3) + \frac{\partial N_i^U}{\partial r}\bar{\theta}_n(3,3)\beta_4\frac{N_j^U}{r}\frac{\partial\bar{\bar{\theta}}_n(3,3)}{\partial\theta} + \frac{N_i^U}{r}\frac{\partial\bar{\theta}_n(3,3)}{\partial\theta}\beta_5\frac{\partial N_j^U}{\partial z}\bar{\bar{\theta}}_n(3,3) + \frac{\partial N_i^U}{\partial z}\bar{\theta}_n(3,3)\beta_5\frac{N_j^U}{r}\frac{\partial\bar{\bar{\theta}}_n(3,3)}{\partial\theta} + \frac{\partial N_i^U}{\partial r}\bar{\theta}_n(3,3)\beta_6\frac{\partial N_j^U}{\partial z}\bar{\bar{\theta}}_n(3,3) + \frac{\partial N_i^U}{\partial z}\bar{\theta}_n(3,3)\beta_6\frac{\partial N_j^U}{\partial r}\bar{\bar{\theta}}_n(3,3)$$

$$C_{ij}(1,1) = \frac{\partial N_i^U}{\partial r}\bar{\bar{\theta}}_n(1,1)\beta_1\frac{\partial N_j^U}{\partial r}\bar{\theta}_n(1,1) + \frac{N_i^U}{r}\bar{\bar{\theta}}_n(1,1)\beta_2\frac{N_j^U}{r}\bar{\theta}_n(1,1) + \frac{N_i^U}{r}\frac{\partial\bar{\bar{\theta}}_n(1,1)}{\partial\theta}\beta_2\frac{N_j^U}{r}\frac{\partial\bar{\theta}_n(1,1)}{\partial\theta} + \frac{\partial N_i^U}{\partial z}\bar{\bar{\theta}}_n(1,1)\beta_3\frac{\partial N_j^U}{\partial z}\bar{\theta}_n(1,1) + \frac{N_i^U}{r}\frac{\partial\bar{\bar{\theta}}_n(1,1)}{\partial\theta}\beta_4\frac{\partial N_j^U}{\partial r}\bar{\theta}_n(1,1) + \frac{\partial N_i^U}{\partial r}\bar{\bar{\theta}}_n(1,1)\beta_4\frac{N_j^U}{r}\frac{\partial\bar{\theta}_n(1,1)}{\partial\theta} + \frac{N_i^U}{r}\frac{\partial\bar{\bar{\theta}}_n(1,1)}{\partial\theta}\beta_5\frac{\partial N_j^U}{\partial z}\bar{\theta}_n(1,1) + \frac{\partial N_i^U}{\partial z}\bar{\bar{\theta}}_n(1,1)\beta_5\frac{N_j^U}{r}\frac{\partial\bar{\theta}_n(1,1)}{\partial\theta} + \frac{\partial N_i^U}{\partial r}\bar{\bar{\theta}}_n(1,1)\beta_6\frac{\partial N_j^U}{\partial z}\bar{\theta}_n(1,1) + \frac{\partial N_i^U}{\partial z}\bar{\bar{\theta}}_n(1,1)\beta_6\frac{\partial N_j^U}{\partial r}\bar{\theta}_n(1,1)$$

$$C_{ij}(2,1) = \frac{N_i^U}{r}\bar{\bar{\theta}}_n(1,1)\beta_2\frac{N_j^U}{r}\frac{\partial\bar{\theta}_n(2,2)}{\partial\theta} - \frac{N_i^U}{r}\frac{\partial\bar{\bar{\theta}}_n(1,1)}{\partial\theta}\beta_2\frac{N_j^U}{r}\bar{\theta}_n(2,2) + \frac{N_i^U}{r}\bar{\bar{\theta}}_n(1,1)\beta_4\frac{\partial N_j^U}{\partial r}\bar{\theta}_n(2,2) - \frac{\partial N_i^U}{\partial r}\bar{\bar{\theta}}_n(1,1)\beta_4\frac{N_j^U}{r}\bar{\theta}_n(2,2) + \frac{N_i^U}{r}\bar{\bar{\theta}}_n(1,1)\beta_5\frac{\partial N_j^U}{\partial z}\bar{\theta}_n(2,2) - \frac{\partial N_i^U}{\partial z}\bar{\bar{\theta}}_n(1,1)\beta_5\frac{N_j^U}{r}\bar{\theta}_n(2,2)$$

$$C_{ij}(2,1) = -\frac{N_i^U}{r}\bar{\bar{\theta}}_n(2,2)\beta_2\frac{N_j^U}{r}\frac{\partial\bar{\theta}_n(1,1)}{\partial\theta} + \frac{N_i^U}{r}\frac{\partial\bar{\bar{\theta}}_n(2,2)}{\partial\theta}\beta_2\frac{N_j^U}{r}\bar{\theta}_n(1,1) - \frac{N_i^U}{r}\bar{\bar{\theta}}_n(2,2)\beta_4\frac{\partial N_j^U}{\partial r}\bar{\theta}_n(1,1) + \frac{\partial N_i^U}{\partial r}\bar{\bar{\theta}}_n(2,2)\beta_4\frac{N_j^U}{r}\bar{\theta}_n(1,1) - \frac{N_i^U}{r}\bar{\bar{\theta}}_n(2,2)\beta_5\frac{\partial N_j^U}{\partial z}\bar{\theta}_n(1,1) + \frac{\partial N_i^U}{\partial z}\bar{\bar{\theta}}_n(2,2)\beta_5\frac{N_j^U}{r}\bar{\theta}_n(1,1)$$

$$C_{ij}(2,2) = \frac{\partial N_i^U}{\partial r}\bar{\bar{\theta}}_n(2,2)\beta_1\frac{\partial N_j^U}{\partial r}\bar{\bar{\theta}}_n(2,2) + \frac{N_i^U}{r}\bar{\bar{\theta}}_n(2,2)\beta_2\frac{N_j^U}{r}\bar{\bar{\theta}}_n(2,2) + \frac{N_i^U}{r}\frac{\partial\bar{\bar{\theta}}_n(2,2)}{\partial\theta}\beta_2\frac{N_j^U}{r}\frac{\partial\bar{\bar{\theta}}_n(2,2)}{\partial\theta} + \frac{\partial N_i^U}{\partial z}\bar{\bar{\theta}}_n(2,2)\beta_3\frac{\partial N_j^U}{\partial z}\bar{\bar{\theta}}_n(2,2) + \frac{N_i^U}{r}\frac{\partial\bar{\bar{\theta}}_n(2,2)}{\partial\theta}\beta_4\frac{\partial N_j^U}{\partial r}\bar{\bar{\theta}}_n(2,2) + \frac{\partial N_i^U}{\partial r}\bar{\bar{\theta}}_n(2,2)\beta_4\frac{N_j^U}{r}\frac{\partial\bar{\bar{\theta}}_n(2,2)}{\partial\theta} + \frac{N_i^U}{r}\frac{\partial\bar{\bar{\theta}}_n(2,2)}{\partial\theta}\beta_5\frac{\partial N_j^U}{\partial z}\bar{\bar{\theta}}_n(2,2) + \frac{\partial N_i^U}{\partial z}\bar{\bar{\theta}}_n(2,2)\beta_5\frac{N_j^U}{r}\frac{\partial\bar{\bar{\theta}}_n(2,2)}{\partial\theta} + \frac{\partial N_i^U}{\partial r}\bar{\bar{\theta}}_n(2,2)\beta_6\frac{\partial N_j^U}{\partial z}\bar{\bar{\theta}}_n(2,2) + \frac{\partial N_i^U}{\partial z}\bar{\bar{\theta}}_n(2,2)\beta_6\frac{\partial N_j^U}{\partial r}\bar{\bar{\theta}}_n(2,2)$$

$$C_{ij}(3,3) = \frac{\partial N_i^U}{\partial r}\bar{\bar{\theta}}_n(3,3)\beta_1\frac{\partial N_j^U}{\partial r}\bar{\theta}_n(3,3) + \frac{N_i^U}{r}\frac{\partial\bar{\bar{\theta}}_n(3,3)}{\partial\theta}\beta_2\frac{N_j^U}{r}\frac{\partial\bar{\theta}_n(3,3)}{\partial\theta} + \frac{\partial N_i^U}{\partial z}\bar{\bar{\theta}}_n(3,3)\beta_3\frac{\partial N_j^U}{\partial z}\bar{\theta}_n(3,3) + \frac{N_i^U}{r}\frac{\partial\bar{\bar{\theta}}_n(3,3)}{\partial\theta}\beta_4\frac{\partial N_j^U}{\partial r}\bar{\theta}_n(3,3) + \frac{\partial N_i^U}{\partial r}\bar{\bar{\theta}}_n(3,3)\beta_4\frac{N_j^U}{r}\frac{\partial\bar{\theta}_n(3,3)}{\partial\theta} + \frac{N_i^U}{r}\frac{\partial\bar{\bar{\theta}}_n(3,3)}{\partial\theta}\beta_5\frac{\partial N_j^U}{\partial z}\bar{\theta}_n(3,3) + \frac{\partial N_i^U}{\partial z}\bar{\bar{\theta}}_n(3,3)\beta_5\frac{N_j^U}{r}\frac{\partial\bar{\theta}_n(3,3)}{\partial\theta} + \frac{\partial N_i^U}{\partial r}\bar{\bar{\theta}}_n(3,3)\beta_6\frac{\partial N_j^U}{\partial z}\bar{\theta}_n(3,3) + \frac{\partial N_i^U}{\partial z}\bar{\bar{\theta}}_n(3,3)\beta_6\frac{\partial N_j^U}{\partial r}\bar{\theta}_n(3,3)$$

$$D_{ij}(1,1) = \frac{\partial N_i^U}{\partial r}\bar{\bar{\theta}}_n(1,1)\beta_1\frac{\partial N_j^U}{\partial r}\bar{\bar{\theta}}_n(1,1) + \frac{N_i^U}{r}\bar{\bar{\theta}}_n(1,1)\beta_2\frac{N_j^U}{r}\bar{\bar{\theta}}_n(1,1) + \frac{N_i^U}{r}\frac{\partial\bar{\bar{\theta}}_n(1,1)}{\partial\theta}\beta_2\frac{N_j^U}{r}\frac{\partial\bar{\bar{\theta}}_n(1,1)}{\partial\theta} + \frac{\partial N_i^U}{\partial z}\bar{\bar{\theta}}_n(1,1)\beta_3\frac{\partial N_j^U}{\partial z}\bar{\bar{\theta}}_n(1,1) + \frac{N_i^U}{r}\frac{\partial\bar{\bar{\theta}}_n(1,1)}{\partial\theta}\beta_4\frac{\partial N_j^U}{\partial r}\bar{\bar{\theta}}_n(1,1) + \frac{\partial N_i^U}{\partial r}\bar{\bar{\theta}}_n(1,1)\beta_4\frac{N_j^U}{r}\frac{\partial\bar{\bar{\theta}}_n(1,1)}{\partial\theta} + \frac{N_i^U}{r}\frac{\partial\bar{\bar{\theta}}_n(1,1)}{\partial\theta}\beta_5\frac{\partial N_j^U}{\partial z}\bar{\bar{\theta}}_n(1,1) + \frac{\partial N_i^U}{\partial z}\bar{\bar{\theta}}_n(1,1)\beta_5\frac{N_j^U}{r}\frac{\partial\bar{\bar{\theta}}_n(1,1)}{\partial\theta} + \frac{\partial N_i^U}{\partial r}\bar{\bar{\theta}}_n(1,1)\beta_6\frac{\partial N_j^U}{\partial z}\bar{\bar{\theta}}_n(1,1) + \frac{\partial N_i^U}{\partial z}\bar{\bar{\theta}}_n(1,1)\beta_6\frac{\partial N_j^U}{\partial r}\bar{\bar{\theta}}_n(1,1)$$

$$D_{ij}(1,2) = \frac{N_i^U}{r}\bar{\bar{\theta}}_n(1,1)\beta_2\frac{N_j^U}{r}\frac{\partial\bar{\bar{\theta}}_n(2,2)}{\partial\theta} - \frac{N_i^U}{r}\frac{\partial\bar{\bar{\theta}}_n(1,1)}{\partial\theta}\beta_2\frac{N_j^U}{r}\bar{\bar{\theta}}_n(2,2) + \frac{N_i^U}{r}\bar{\bar{\theta}}_n(1,1)\beta_4\frac{\partial N_j^U}{\partial r}\bar{\bar{\theta}}_n(2,2) - \frac{\partial N_i^U}{\partial r}\bar{\bar{\theta}}_n(1,1)\beta_4\frac{N_j^U}{r}\bar{\bar{\theta}}_n(2,2) + \frac{N_i^U}{r}\bar{\bar{\theta}}_n(1,1)\beta_5\frac{\partial N_j^U}{\partial z}\bar{\bar{\theta}}_n(2,2) - \frac{\partial N_i^U}{\partial z}\bar{\bar{\theta}}_n(1,1)\beta_5\frac{N_j^U}{r}\bar{\bar{\theta}}_n(2,2)$$

$$D_{ij}(2,1) = -\frac{N_i^U}{r}\bar{\bar{\theta}}_n(2,2)\beta_2\frac{N_j^U}{r}\frac{\partial\bar{\bar{\theta}}_n(1,1)}{\partial\theta} + \frac{N_i^U}{r}\frac{\partial\bar{\bar{\theta}}_n(2,2)}{\partial\theta}\beta_2\frac{N_j^U}{r}\bar{\bar{\theta}}_n(1,1) - \frac{N_i^U}{r}\bar{\bar{\theta}}_n(2,2)\beta_4\frac{\partial N_j^U}{\partial r}\bar{\bar{\theta}}_n(1,1) + \frac{\partial N_i^U}{\partial r}\bar{\bar{\theta}}_n(2,2)\beta_4\frac{N_j^U}{r}\bar{\bar{\theta}}_n(1,1) - \frac{N_i^U}{r}\bar{\bar{\theta}}_n(2,2)\beta_5\frac{\partial N_j^U}{\partial z}\bar{\bar{\theta}}_n(1,1) + \frac{\partial N_i^U}{\partial z}\bar{\bar{\theta}}_n(2,2)\beta_5\frac{N_j^U}{r}\bar{\bar{\theta}}_n(1,1)$$

$$D_{ij}(2,2) = \frac{\partial N_i^U}{\partial r}\bar{\bar{\theta}}_n(2,2)\beta_1\frac{\partial N_j^U}{\partial r}\bar{\bar{\theta}}_n(2,2) + \frac{N_i^U}{r}\bar{\bar{\theta}}_n(2,2)\beta_2\frac{N_j^U}{r}\bar{\bar{\theta}}_n(2,2) + \frac{N_i^U}{r}\frac{\partial\bar{\bar{\theta}}_n(2,2)}{\partial\theta}\beta_2\frac{N_j^U}{r}\frac{\partial\bar{\bar{\theta}}_n(2,2)}{\partial\theta} + \frac{\partial N_i^U}{\partial z}\bar{\bar{\theta}}_n(2,2)\beta_3\frac{\partial N_j^U}{\partial z}\bar{\bar{\theta}}_n(2,2) + \frac{N_i^U}{r}\frac{\partial\bar{\bar{\theta}}_n(2,2)}{\partial\theta}\beta_4\frac{\partial N_j^U}{\partial r}\bar{\bar{\theta}}_n(2,2) + \frac{\partial N_i^U}{\partial r}\bar{\bar{\theta}}_n(2,2)\beta_4\frac{N_j^U}{r}\frac{\partial\bar{\bar{\theta}}_n(2,2)}{\partial\theta} + \frac{N_i^U}{r}\frac{\partial\bar{\bar{\theta}}_n(2,2)}{\partial\theta}\beta_5\frac{\partial N_j^U}{\partial z}\bar{\bar{\theta}}_n(2,2) + \frac{\partial N_i^U}{\partial z}\bar{\bar{\theta}}_n(2,2)\beta_5\frac{N_j^U}{r}\frac{\partial\bar{\bar{\theta}}_n(2,2)}{\partial\theta} + \frac{\partial N_i^U}{\partial r}\bar{\bar{\theta}}_n(2,2)\beta_6\frac{\partial N_j^U}{\partial z}\bar{\bar{\theta}}_n(2,2) + \frac{\partial N_i^U}{\partial z}\bar{\bar{\theta}}_n(2,2)\beta_6\frac{\partial N_j^U}{\partial r}\bar{\bar{\theta}}_n(2,2)$$

$$D_{ij}(3,3) = \frac{\partial N_i^U}{\partial r}\bar{\bar{\theta}}_n(3,3)\beta_1\frac{\partial N_j^U}{\partial r}\bar{\bar{\theta}}_n(3,3) + \frac{N_i^U}{r}\frac{\partial\bar{\bar{\theta}}_n(3,3)}{\partial\theta}\beta_2\frac{N_j^U}{r}\frac{\partial\bar{\bar{\theta}}_n(3,3)}{\partial\theta} + \frac{\partial N_i^U}{\partial z}\bar{\bar{\theta}}_n(3,3)\beta_3\frac{\partial N_j^U}{\partial z}\bar{\bar{\theta}}_n(3,3)$$

$$+\frac{N_i^U}{r}\frac{\partial\bar{\bar{\theta}}_n(3,3)}{\partial\theta}\beta_4\frac{\partial N_j^U}{\partial r}\bar{\bar{\theta}}_n(3,3)+\frac{\partial N_i^U}{\partial r}\bar{\bar{\theta}}_n(3,3)\beta_4\frac{N_j^U}{r}\frac{\partial\bar{\bar{\theta}}_n(3,3)}{\partial\theta}$$
$$+\frac{N_i^U}{r}\frac{\partial\bar{\bar{\theta}}_n(3,3)}{\partial\theta}\beta_5\frac{\partial N_j^U}{\partial z}\bar{\bar{\theta}}_n(3,3)$$
$$+\frac{\partial N_i^U}{\partial z}\bar{\bar{\theta}}_n(3,3)\beta_5\frac{N_j^U}{r}\frac{\partial\bar{\bar{\theta}}_n(3,3)}{\partial\theta}$$
$$+\frac{\partial N_i^U}{\partial r}\bar{\bar{\theta}}_n(3,3)\beta_6\frac{\partial N_j^U}{\partial z}\bar{\bar{\theta}}_n(3,3)$$
$$+\frac{\partial N_i^U}{\partial z}\bar{\bar{\theta}}_n(3,3)\beta_6\frac{\partial N_j^U}{\partial r}\bar{\bar{\theta}}_n(3,3)$$

Appendix E

$$T_u=\begin{bmatrix}\psi_1(\mathrm{r}_1,\mathrm{z}_1) & 0 & 0 & \psi_n(\mathrm{r}_1,\mathrm{z}_1) & 0 & 0\\ 0 & \psi_1(\mathrm{r}_1,\mathrm{z}_1) & 0 & 0 & \psi_n(\mathrm{r}_1,\mathrm{z}_1) & 0\\ 0 & 0 & \psi_1(\mathrm{r},\mathrm{z}) & 0 & 0 & \psi_n(\mathrm{r}_1,\mathrm{z}_1)\\ \vdots & \vdots & \vdots & \cdots\ \vdots & \vdots & \vdots\\ \psi_1(\mathrm{r}_n,\mathrm{z}_n) & 0 & 0 & \psi_n(\mathrm{r}_n,\mathrm{z}_n) & 0 & 0\\ 0 & \psi_1(\mathrm{r}_n,\mathrm{z}_n) & 0 & 0 & \psi_n(\mathrm{r}_n,\mathrm{z}_n) & 0\\ 0 & 0 & \psi_1(\mathrm{r}_n,\mathrm{z}_n) & 0 & 0 & \psi_n(\mathrm{r}_n,\mathrm{z}_n)\end{bmatrix}$$

$$T_\Phi=\begin{bmatrix}\psi_1(\mathrm{r}_1,\mathrm{z}_1) & \psi_2(\mathrm{r}_1,\mathrm{z}_1) & \cdots & \psi_n(\mathrm{r}_1,\mathrm{z}_1)\\ \psi_1(\mathrm{r}_2,\mathrm{z}_2) & \psi_2(\mathrm{r}_2,\mathrm{z}_2) & \cdots & \psi_n(\mathrm{r}_2,\mathrm{z}_2)\\ \vdots & \vdots & & \vdots\\ \psi_1(\mathrm{r}_n,\mathrm{z}_n) & \psi_2(\mathrm{r}_n,\mathrm{z}_n) & \cdots & \psi_n(\mathrm{r}_n,\mathrm{z}_n)\end{bmatrix}$$

Appendix F

$$N_U(\mathrm{r},\mathrm{z})=\begin{bmatrix}\psi_1(\mathrm{r},\mathrm{z}) & 0 & 0 & \psi_2(\mathrm{r},\mathrm{z}) & 0 & 0 & \cdots & \psi_n(\mathrm{r},\mathrm{z}) & 0 & 0\\ 0 & \psi_1(\mathrm{r},\mathrm{z}) & 0 & 0 & \psi_2(\mathrm{r},\mathrm{z}) & 0 & \cdots & 0 & \psi_n(\mathrm{r},\mathrm{z}) & 0\\ 0 & 0 & \psi_1(\mathrm{r},\mathrm{z}) & 0 & 0 & \psi_2(\mathrm{r},\mathrm{z}) & \cdots & 0 & 0 & \psi_n(\mathrm{r},\mathrm{z})\end{bmatrix}$$